The Kinematic State of the Local Volume

Alan B. Whiting

Cerro Tololo Interamerican Observatory

whiting@ctio.noao.edu

ABSTRACT

The kinematics of galaxies with 10 megaparsecs (10 Mpc) of the Milky Way is investigated using published distances and radial velocities. With respect to the average Hubble flow (isotropic or simple anisotropic), there is no systematic relation between peculiar velocity dispersion and absolute magnitude over a range of 10 magnitudes; neither is there any apparent variation with galaxy type or between field and cluster members. There are several possible explanations for the lack of variation, though all have difficulties: either there is no relationship between light and mass on these scales, or the peculiar velocities are not produced by gravitational interaction, or the background dynamical picture is wrong in some systematic way. The extremely cold local flow of 40-60 km s⁻¹ dispersion reported by some authors is shown to be an artifact of sparse data, a velocity dispersion of over 100 km s⁻¹ being closer to the actual value. Galaxies with a high (positive) radial velocity have been selected against in studies of this volume, biasing numerical results.

Subject headings: galaxies: kinematics and dynamics—cosmological parameters—cosmology: observations—dark matter

1. Mass and Motion Models

Under the physically well-motivated assumption that the only important force on the largest astronomical scales and for most of the history of the universe is gravity, there should be an intimate relationship between the cosmic velocity field and the cosmic density field. Predicting, calculating and observing the details of this relationship have been the major occupations of cosmology for most of the past century.

The first-order description of the kinematics of the universe takes the form of a homogeneous, isotropic expansion. To investigate this it is best to examine the largest spatial scales,

where the density field is closest to the homogeneous ideal. In that case the observational goal is to determine the Hubble constant (H_0) and the major problem is the determination of reliable distances. A subsidiary problem appears in practice, seen for example in de Vaucouleurs & Bollinger (1979), in the fact that the distribution of galaxies with the most reliable distances (the closer ones) is not homogeneous and their motions are subsequently not uniform.

With improving observational and calculational techniques this subsidary problem has been turned into an area of research in its own right. Courteau, Strauss, & Willick (2000) provide an overview; specific techniques and results are found in, for instance, Branchini et al. (1999) and Dekel et al. (1999). One of the objects of this work is the estimations of the biasing parameter, which measures the relationship between actual density fluctuations and observed galaxies. To do this convincingly, however, requires a volume large enough that density contrasts remain in or near the linear region, hence this is the study of large-scale structure. Unfortunately, distance indicators for galaxies so far away are not very accurate and are subject to various systematic biases; one must take large samples and be careful about manipulating statistics.

The situation reverses itself in the Local Volume, the region within about 10 megaparsecs (Mpc). Here we are several rungs down on the cosmic distance ladder and distance indicators are based on resolved stars, allowing accuracies better than 7% under good conditions. With redshifts good to a few km s⁻¹ from HI observations, the data are (potentially) excellent. Balancing this are the complications of nonlinear dynamics (sufficiently nonlinear that pertubative techniques, such as the Zeldovich approximation and expansion to a few orders, cannot be used) and the fact that peculiar velocities are comparable to the Hubble flow.

Dynamically, this is almost unknown territory. It lies between the well-studied galaxy and galaxy group scales on one hand, and that of large-scale structure on the other. Neither are there any galaxy clusters in the Local Volume, Virgo being just outside. The potential scientific returns of examining this unexplored region, especially when excellent data are available, are great. For instance, dark matter on galaxy scales seems to be concentric with luminous matter, but far more extended; on the linear-structure scale, both seem to be distributed the same way. The biasing parameter b, which measures the concentration of luminous matter relative to dark matter, is found to be in the range 0.5-1.0 on large scales (Dekel et al. (1999); Branchini et al. (1999)); within a spiral galaxy it must range from zero beyond the visible disk to some number possibly greater than unity at the center. In between these two scales, what happens?

Without a dynamical model of obvious applicability to the Local Volume, we must begin

by studying the kinematics. The procedure in what follows is to calculate overall average motions, and then examine deviations from them for systematic effects. In effect, we are looking for some kind of non-randomness among peculiar (radial) velocities.

Two models will be used for the "overall average motions." Both include the average velocity of all galaxies in a sample, showing up as the solar reflex velocity; the first model then adds a uniform expansion (the local reflection of the universal Hubble flow). The second is suggested by the general distribution of galaxies within the Volume. The Supergalactic Plane is well-defined in this region, clear in Tully & Fisher (1987) as well as with updated data in Karachentsev & Makarov (1996) and Lahav et al. (2000). There should be therefore an anisotropy in the overall flow, expansion normal to the Supergalactic Plane being slower than in the Plane. In fact de Vaucouleurs & Bollinger (1979) found something of the sort, as have Karachentsev & Makarov (2001) and Karachentsev & Makarov (1996). In addition, the tidal effect of the Virgo Cluster should be visible as an elongation (high eigenvalue) in the direction of the Cluster and a contraction (low eigenvalues) normal to it. Since Virgo is almost in the Plane, at roughly Supergalactic Longitude 100°, we expect the highest eigenvalue in that direction, the lowest at the Supergalactic poles, and an intermediate eigenvalue in the Plane at longitude about 10°. This relationship between the distribution of galaxies in the Supergalactic Plane and velocities can be seen either as dynamic (the concentration of mass causing anisotropic motions) or as kinematic (the concentration of galaxies having been produced by anisotropic motions), or more accurately both.

2. The Overall Hubble Flow

2.1. Calculations

The mathematical tools used here are similar to some of those developed in Lynden-Bell et al. (1988), though details and the use to which they are put differ.

Suppose that the velocity field in the Local Volume is smooth, continuous and differentiable. Under these conditions we may expand this field in terms of the vector distance from us, \mathbf{r} , as a Taylor series:

$$\mathbf{v} = \mathbf{v}_0 + \mathbf{r} \cdot \frac{\partial \mathbf{v}}{\partial \mathbf{r}} + \frac{1}{2} \mathbf{r} \cdot \frac{\partial^2 \mathbf{v}}{\partial \mathbf{r}^2} \cdot \mathbf{r} + \cdots$$
 (1)

If we truncate this series at the term linear in distance and recognize that only the radial velocities are observable, we find that

$$v_{\text{obs}} = \mathbf{v} \cdot \hat{\mathbf{r}} = \mathbf{v}_0 \cdot \hat{\mathbf{r}} + \mathbf{r} \cdot \mathbf{H} \cdot \hat{\mathbf{r}}$$
 (2)

where \mathbf{H} is the symbol for the first-order partial-derivative tensor and $\hat{\mathbf{r}}$ is the unit vector in the \mathbf{r} direction. If the tensor is isotropic, \mathbf{H} reduces to a scalar; if the region over which it is determined is representative of the universe as a whole, it is the Hubble constant. It is therefore convenient to call \mathbf{H} the Hubble tensor¹. The Hubble tensor, quantifying anisotropic motion, is the next more complicated description of cosmic motion after a simple uniform expansion.

To determine the components of the Hubble tensor from a set of data, a least-squares method is the most straightforward. We take as a measure of goodness of fit the average square of the difference between the predicted radial velocity and the observed radial velocity²,

$$\sigma^2 = \frac{1}{N} \sum_{i} \sigma_i^2 = \frac{1}{N} \sum_{i} \left(v_{\text{obs}} - (\mathbf{v}_0 \cdot \hat{\mathbf{r}} + \hat{\mathbf{r}} \cdot \mathbf{H} \cdot \mathbf{r}) \right)^2$$
 (3)

Taking the derivatives of this with respect to the three components of \mathbf{v}_0 and the six independent components of \mathbf{H} and setting them equal to zero gives nine linear equations to be solved for the nine unknowns, a straightforward if tedious calculation³. An isotropic solution is determined similarly, using four equations in four unknowns.

2.2. Data

Distance and radial velocity data for galaxies within 10 Mpc were gathered from the literature and are summarized in Table 1. In gathering the data much use has been made of the NASA/IPAC Extragalactic Database (NED)⁴. The column headings are: (1) Designation; for those galaxies which have been catalogued several times, only one was chosen, to maintain readability of the table⁵; (2) Apparent B magnitude, from NED; (3) Morphological type, from NED; (4) Supergalactic longitude, in degrees; (5) Supergalactic latitude, in degrees; (6) Radial velocity, in km s⁻¹; (7) the source for the radial velocity; (8) Distance,

¹However, it is worth emphasizing that the determination of the Hubble tensor over the Local Volume has no necessary cosmic implication, since this region is too small to be a fair sample of the universe.

 $^{^2\}mathrm{Compare}$ Karachentsev & Makarov (2001), in which a slightly different measure is used.

³In practice, this was done by the Mathematica program.

⁴NED is operated by the Jet Propulsion Laboratory, California Institute of Technology, under contract with the National Aeronautics and Space Administration.

⁵Unfortunately, most galaxies in this sample have at least three popular designations, and a given author will mention one while another will only use a different one. The designation used here is generally that found in the distance reference; others may conveniently be found by referring to NED.

in Mpc; (9) the source for the distance; (10) the method used to derive the distance. The references corresponding to the source codes are listed at the end of the table. An asterisk denotes data which are not known.

Galaxies known to be part of the Local Group are not included, to avoid a possible dynamical bias at the small end of the distance scale. Of course, distances derived from a velocity model were of no use for this purpose. Those available were based on Cepheids ("ceph" in the table), brightness of the tip of the Red Giant Branch (TRGB; in one case, the tip of the Asymptotic Giant Branch, TAGB), surface brightness fluctuations (SBF), a geometric method involving water masers (geo), or the brightness of the brightest stars (stars). The former methods have quoted accuracies of \pm 0.2 magnitudes or less in distance modulus. The last method was found by Karachentsev & Tikhonov (1994) to have an accuracy of 0.3 to 0.45 magnitudes, depending on exactly how it was applied. However, in several cases (see, for example, Crone et al. (2000), and compare Karachentsev & Makarov (1996) with Aparicio & Tikhonov (2000) for the case of DDO 109 = UGC 9240) it has been found to be in error by a factor of two or more. In what follows calculations will be performed separately on both on the full data set of 98 galaxies (so as to take advantage of the larger number of objects) and on the set of 35 galaxies with more reliable distances.

Although the data come from many sources and some difficulties could be anticipated from that fact, in practice there were no problems along those lines. Each of the TRGB distances used the same calibration (Lee, Freedman & Madore 1993), as did the Cepheid distances within the stated errors; and all used as a zero-point the Large Magellanic Cloud at a distance modulus of 18.50. The SBF method itself was calibrated using TRGB and Cepheid data, most of which found its way into this data set. The internal consistency of the better-quality distances is therefore reliable⁶.

As noted, the brightest-star distances are treated with less confidence here, and the better-quality data will be examined separately when possible. In the case of NGC 4258 the Cepheid and geometric distances do not agree within their stated errors (7.98 and 7.2 Mpc, respectively). The distance shown is the average.

It is worth pointing out that the data amount to a minority of the galaxies estimated to lie in this volume. Including the brightest-star galaxies possibly as much as a quarter of the population is represented; restricting ourselves to the better data, less than a tenth⁷. In

⁶This agreeable state of affairs probably won't last long, as someone is sure to come up with a "better" calibration of some distance method soon.

⁷So even if one were to ignore nonlinear effects, a POTENT-like treatment (Dekel et al. 1999) of the Local Volume is impossible: the locations of most of the luminous masses are just not known.

addition, these are not all the largest or brightest, nor uniformly distributed. It is worthwhile, then, to look into possible effects of this uneven sampling.

The average motion of all the galaxies in each sample will show up in the solar reflex velocity. Subsidiary "bulk flows," motions of one part of the Volume with respect to the whole, will appear as peculiar velocities systematically different in that part—but only if there are galaxies there to show it. Similarly, flows on a smaller scale (or a larger) than is sampled will go unnoticed.

More subtle would be effects on overall parameters due to badly-distributed data. To examine those, suppose that we are attempting to fit a model of anisotropic flow (as above) to an actual flow. The "real" flow is described by a flow with noise, in part due to distance errors (which obey a distribution function δr) and in part due to real peculiar velocities (which obey a vector distribution function \mathbf{e}). The quantity we attempt to minimize during least-squares fitting is then

$$\sigma^{2} = \frac{1}{N} \sum_{i} (v_{obs} - v_{model})^{2}$$

$$= \frac{1}{N} \sum_{i} (\mathbf{v}_{0a} \cdot \hat{\mathbf{r}}_{i} + \hat{\mathbf{r}}_{i} \cdot \mathbf{H}_{a} \cdot \hat{\mathbf{r}}_{i} (r_{i} + \delta r_{i}) + \mathbf{e}_{i} \cdot \hat{\mathbf{r}}_{i} - \mathbf{v}_{0m} \cdot \hat{\mathbf{r}}_{i} - \hat{\mathbf{r}}_{i} \cdot \mathbf{H}_{m} \cdot \hat{\mathbf{r}}_{i} r_{i})^{2}$$

where the subscript a stands for "actual" and m for "model," and the vector \mathbf{r} is written as a product of magnitude and direction, $r\hat{\mathbf{r}}$. The various terms may be regrouped as follows:

$$\sigma^{2} = \frac{1}{N} \sum_{i} \left[((\mathbf{v}_{0a} - \mathbf{v}_{0m}) \cdot \hat{\mathbf{r}}_{i} + \hat{\mathbf{r}}_{i} \cdot (\mathbf{H}_{a} - \mathbf{H}_{m}) \cdot \hat{\mathbf{r}}_{i} r_{i})^{2} \right]$$

$$+ 2 (\mathbf{v}_{0a} - \mathbf{v}_{0m}) \cdot \hat{\mathbf{r}}_{i} \hat{\mathbf{r}}_{i} \cdot \mathbf{H}_{a} \cdot \hat{\mathbf{r}}_{i} \delta r_{i}$$

$$+ 2 \hat{\mathbf{r}}_{i} \cdot (\mathbf{H}_{a} - \mathbf{H}_{m}) \cdot \hat{\mathbf{r}}_{i} r_{i} \hat{\mathbf{r}}_{i} \cdot \mathbf{H}_{a} \cdot \hat{\mathbf{r}}_{i} \delta r_{i}$$

$$+ 2 \hat{\mathbf{r}}_{i} \cdot (\mathbf{H}_{a} - \mathbf{H}_{m}) \cdot \hat{\mathbf{r}}_{i} r_{i} e_{i} \cdot \hat{\mathbf{r}}_{i}$$

$$+ 2 (\mathbf{v}_{0a} - \mathbf{v}_{0m}) \cdot \hat{\mathbf{r}}_{i} e_{i} \cdot \hat{\mathbf{r}}_{i}$$

$$+ (\hat{\mathbf{r}}_{i} \cdot \mathbf{H}_{a} \cdot \hat{\mathbf{r}}_{i} \delta r_{i} + e_{i} \cdot \hat{\mathbf{r}}_{i})^{2}$$

The first line, the squared term, is the difference between the model and the actual situation in the absence of errors or noise; its minimum is zero, when the actual and model parameters are identical. The last line is the collected "noise" and does not contain the model parameters at all; its only effect on the process is to set a positive minimum to the quantity σ^2 . The cross terms require some attention.

If we assume that the real peculiar velocity distribution \mathbf{e} does not depend on direction or distance, the two cross terms containing it will average to zero. Also, if the distance errors δr_i do not depend on direction (that is, our measures are no more uncertain in one part of

the sky than another), the first cross term vanishes also. The second cross term is harder to deal with, since in general we do expect a correlation between the distance r_i and the distance error δr_i : the distance error should be larger as the distance itself increases, so that galaxies farther away will contribute terms of larger magnitude to this sum. However, as long as the error distribution function itself averages to zero, this cross term also vanishes.

So if peculiar velocities and distance errors have no systematic correlation with direction then the actual distribution of galaxies (the particular \mathbf{r}_i from which kinematic model parameters are derived) is irrelevant. The lack of galaxies at high Supergalactic latitudes, for instance, and in some directions in the Supergalactic Plane should not bias the values for the solar reflex velocity and Hubble tensor. Put another way, if all the galaxies in the sample take part in the same motion with random deviations, the motion can be reconstructed from any part of it (though with varying amounts of uncertainty).

A peculiar velocity distribution which does show some systematic variation with position, of course, will change the derived overall parameters. In the simplest case it would be a sort of "bulk flow" on a smaller scale than the total sample, and should be visible in plots of peculiar velocity against position (which will be shown below). In the case of a mass concentration like a cluster, a locally increased velocity dispersion should be visible on the same plots. Of course, in volumes containing few or no sample galaxies such flows or mass concentrations will not be visible.

There remains the possibility of inducing biases by the choice of the galaxy sample. This is potentially serious, since the available data were gathered from many different sources who had obtained them for many different reasons, and there is no guarantee of even coverage in any parameter. An example of subtle biases of this sort is found in Rubin, Ford & Rubin (1973). There, a study of galaxies in a narrow magnitude range showed a significant velocity anisotropy, most evident in two concentrations at 4950 km s⁻¹ and 6400 km s⁻¹. Further analysis (Fall & Jones 1976) showed that the narrow magnitude range actually isolated different parts of the galaxy luminosity function in each case, so in fact different kinds of galaxy were being compared; a further attempt to limit the sample by redshift only exacerbated the problem (James, Joseph & Collins 1991).

The present study is not subject to quite the same kind of bias. The distances used here are not dependent on a certain selection technique for the galaxies, and especially for the higher-accuracy sample are quite good. The range in absolute magnitude is very wide and there is no great concentration in any luminosity interval (to anticipate, see Figures 16 and 17); neither is there a concentration at any particular distance within the 10 Mpc limit (Figure 18). It appears that the hetrogeneous nature of the sample has acted as a sort of random selection, at least in those variables.

There still remains the possibility of a slightly different bias, perhaps stemming from uneven spatial coverage or some effect which causes kinematically important galaxies to be underrepresented in published data. Especially given the fact that a minority of galaxies known to be within this chosen region is represented, it is well to keep this in mind. Unfortunately, it is impossible to correct for a bias whose form (and even existence) is unknown.

Table 1. Local Volume Galaxy Data

Designation	Mag	Type	L	В	RV	RV Source	Dist	Dist Source	Method
A0554+0728	18.4	${ m Im}$	353.90	-62.79	411	KM96	5.50	KM96	stars
Antlia	16.2	dE	139.93	-44.80	361	RC3	1.32	A97	TRGB
BK3N	17.1	Im	41.10	0.40	-40	KMa96	2.79	KMa96	stars
DDO13	14.4	Im	315.26	-6.14	631	RC3	9.04	S96	stars
DDO50	11.1	Im	33.30	-2.40	158	RC3	3.05	H98	ceph
DDO53	14.5	Im	35.90	-6.10	19	RC3	3.08	KMa96	stars
DDO63	13.0	IAB	38.76	1.34	136	RC3	6.95	KT94	stars
DDO66	14.3	Im	41.30	0.70	46	RC3	3.41	KMa96	stars
DDO70	11.8	Im	95.53	-39.62	301	RC3	1.33	S97	TRGB/ceph
DDO71	18.0	Im	43.51	-0.58	-126	NED	3.50	KKD00	TRGB
DDO75	11.9	IBm	109.25	-40.67	324	RC3	1.39	P94	ceph
DDO82	13.5	Sm:	41.69	3.85	40	KMa96	4.48	KMa96	stars
DDO155	14.7	$\mathrm{Im}\mathrm{V}$	103.13	4.66	214	RC3	2.24	T95	ceph
DDO165	12.8	Im	49.60	15.60	37	RC3	4.88	KMa96	stars
DDO187	14.4	ImIV	97.93	24.35	154	RC3	2.50	ATK00	TRGB
DDO190	13.2	IAm	74.10	26.90	156	AT00	2.90	AT00	TRGB
ESO294-G10	15.6	dS0/Im	254.37	-5.27	117	J98	1.71	J98	SBF
IC342	9.1	SAB	10.60	0.37	34	RC3	2.12	KT94	stars
IC4182	13.0	SA	80.22	11.60	321	RC3	4.49	FMG01	ceph
IC2574	10.8	SAB	43.60	2.30	47	RC3	3.78	KMa96	stars
KDG52	16.5	I:	33.52	-1.93	113	KMa96	2.95	KMa96	stars
KDG61	15.6	dE	41.54	0.33	-135	NED	3.60	KKD00	TRGB
KDG73	14.9	Im	44.03	4.75	-132	NED	4.04	KMa96	stars

- 10 -

Designation	Mag	Type	L	В	RV	RV Source	Dist	Dist Source	Method
KK251	16.5	Ir:	10.79	42.12	126	KSH00	5.30	KSH00	stars
KK252	17.1	Sph:	10.97	41.67	132	KSH00	5.30	KSH00	stars
KKR25	17.0	Ir	56.09	40.37	-135	NED	1.86	KSD01b	TRGB
KKR55	17.0	Ir	8.80	41.05	23	NED	5.40	KSH00	stars
KKR56	17.6	Ir	6.94	42.25	-135	NED	6.40	KSH00	stars
KKR59	15.7	Ir	3.74	41.95	17	NED	4.70	KSH00	stars
Maffei1	11.4	S0	359.29	1.44	13	NED	4.40	Dv01	TAGB
NGC59	13.1	SA	273.17	3.16	362	J98	4.39	J98	SBF
NGC300	8.9	SA	259.69	-9.50	142	RC3	2.00	FMG01	ceph
NGC628	9.9	SA	314.88	-5.39	656	RC3	7.32	S96	stars
NGC784	12.2	SBdm:	328.81	-6.31	198	\overline{NED}	5.00	DK00	stars
NGC925	10.7	SAB	335.72	-9.47	553	RC3	9.16	FMG01	ceph
NGC1560	12.2	SA	15.85	0.79	-36	RC3	3.73	KT94	stars
NGC1705	12.8	SA0	231.82	-45.54	628	NED	5.10	TSB01	TRGB
NGC2366	11.4	IB	29.16	-4.86	100	RC3	3.44	TS95	ceph
NGC2403	8.9	SAB	30.50	-8.31	131	RC3	3.22	FMG01	ceph
NGC2683	10.6	SA	55.87	-33.42	411	\overline{NED}	9.20	DK00	stars
NGC2903	9.7	SB	73.53	-36.44	556	NED	8.90	DK00	stars
NGC2976	10.8	SAc	40.98	-0.78	3	RC3	4.57	KMa96	stars
NGC3031	7.9	SA	40.77	0.59	-34	RC3	3.63	FMG01	ceph
NGC3034	9.3	I0	40.38	1.06	203	RC3	3.89	S99	TRGB
NGC3077	10.6	I0	41.51	0.83	14	RC3	3.90	SM01	TRGB
NGC3109	10.4	SB	138.30	-45.10	404	RC3	1.33	M99	ceph

Table 1—Continued

Type Dist Source Designation Mag \mathbf{L} В RV **RV** Source Dist Method NGC3274 -21.80 RC3 8.00 13.2 SAB 77.20537 KMa96 stars -28.57 NGC3621 10.2 727 RC3 SA145.976.64FMG01 ceph NGC4144 68.84 3.83 RC3 Kd9812.1SAB 267 9.70stars NGC4236 10.1 SB46.76 11.38 -5 RC3 3.24 KMa96 stars NGC4244 10.9 SA2.41 RC3Kd9877.58 243 4.50stars NGC4258 H99,FMG01 9.1 SAB 5.55 470 H99 7.60 68.50 geo,ceph NGC4395 RC3 Kd9810.6 SA82.21 2.74320 4.20stars NGC4449 72.09 RC3 2.90 Kd9810.0 IBm6.18 201 stars NGC4523 SAB 100.42 -0.86262 NED 6.40TGD00 stars 14.4NGC4605 SB55.14 12.02 RC3 5.18 KMa96 10.9 143 stars NGC5128 RC3 **TRGB** 7.8 S0159.98 -5.25562 3.63 So96 DK00NGC5204 SA 59.10 17.85 204 RC3 4.10 stars 11.7NGC5236 8.2 SAB 148.25 0.99 516 RC3 4.50KMa96 stars NGC5238 SAB 66.60 18.40 232 RC3 5.18 KMa96 13.9 stars NGC5253 RC3 3.15 FMG01 10.9 150.12 1.00 404 Imceph SAB RC3 NGC5457 8.3 63.30 22.61 241 6.70FMG01 ceph RC3NGC5474 11.3 SA64.03 22.90 277 6.80DK00 stars NGC5477 14.4SA 63.40 22.90 304 RC3 7.73 KMa96 stars NGC5585 11.2 SAB 24.70 305 RC3 8.70 DK0060.40 stars NGC6789 13.8 Im23.27 41.59 -141 DT99 3.60 DSH01 **TRGB** SAB NGC6946 9.6 10.03 42.00 51 KSH00 6.80 KSH00 stars ORION 18.0 SBd 345.25-62.95 365 KM96 6.40 KM96 stars UGC288 16.0 338.00 15.38 RC3 6.73 GKT97 188 Imstars

Table 1—Continued

Table 1—Continued

Designation	Mag	Type	L	В	RV	RV Source	Dist	Dist Source	Method
UGC1104	14.2	Im	317.00	-3.70	669	RC3	7.55	S96	stars
UGC1171	17.0	Im	315.22	-6.04	667	RC3	7.35	S96	stars
UGC2905	15.3	Im	330.78	-35.54	292	NED	5.83	GKT97	stars
UGC3755	14.1	Im	36.82	-63.36	314	NED	4.14	GKT97	stars
UGC3860	15.1	Im	33.96	-33.00	354	\overline{NED}	7.00	GKT97	stars
UGC3966	13.9	Im	37.04	-33.14	361	NED	6.85	GKT97	stars
UGC3974	13.6	IBm	46.54	-55.49	272	\overline{NED}	4.27	GKT97	stars
UGC4115	15.2	IAm	54.21	-56.22	338	NED	5.27	GKT97	stars
UGC4483	15.1	*	34.69	-2.65	156	RC3	3.20	DMK01	TRGB
UGC5721	13.2	SAB	77.24	-21.81	537	NED	7.98	GKT97	stars
UGC6451	16.5	*	64.19	-0.79	249	NED	4.20	SHG00	TRGB
UGC6456	14.5	Р	36.54	11.40	-93	RC3	4.79	LT99	TRGB
UGC6541	*	*	64.19	-0.79	249	NED	3.52	GKT97	stars
UGC6565	12.1	Irr	59.57	1.79	229	RC3	3.52	GKT97	stars
UGC6572	14.3	ImIII	67.96	-2.08	229	NED	3.47	GKT97	stars
UGC6817	13.4	Im	74.93	-2.12	242	NED	3.92	GKT97	stars
UGC7559	14.2	IBm	78.93	4.03	218	RC3	3.93	GKT97	stars
UGC7857	14.7	Sd	102.31	0.63	18	NED	6.30	TGD00	stars
UGC8320	12.7	IBm	71.98	14.55	195	RC3	3.30	KMa96	stars
UGC8331	14.6	IAm	70.37	14.93	260	RC3	8.20	Kd98	stars
UGC8508	14.4	IAm	62.81	17.91	62	RC3	3.68	KMa96	stars
UGC9405	17.0	Im	59.38	26.65	222	RC3	7.62	KMa96	stars
UGC11583	17.0	Irr	10.89	42.07	127	KSH00	8.20	KSH00	stars

Table 1—Continued

Designation	Mag	Type	L	В	RV	RV Source	Dist	Dist Source	Method
UGCA86	13.5	Im:	10.71	-1.18	67	KMa96	1.77	KT94	stars
UGCA92	13.8	Im:	11.18	-6.01	-99	KMa96	2.21	KMa96	stars
UGCA105	13.9	Im:	14.82	-9.26	111	RC3	3.24	KT94	stars
UGCA281	15.2	Sm	67.94	7.06	281	RC3	5.90	SHG01	TRGB
UGCA290	16.0	*	77.94	6.41	445	\overline{NED}	6.70	CSH00	TRGB
UGCA438	13.9	IB	258.88	9.28	62	L78	2.08	LB99	TRGB

Note. — References: A97, Aparicio et al. (1997); AT00, Aparicio & Tikhonov (2000); ATK00, Aparicio, Tikhonov, & Karachentsev (2000); CSH00, Crone et al. (2000); DK00, Drozdovsky & Karachentsev (2000); DMK01, Dolphin et al. (2001); DSH01, Drozdovsky et al. (2001); DT99, Drozdovsky & Tikhonov (1999); Dv01, Davidge & van den Bergh (2001); FMG01, Freedman et al. (2001); GKT97, Georgiev, Karachentsev, & Tikhonov (1997); H98, Hoessel et al. (1998); H99, Herrnstein et al. (1999); J98, Jerjen et al. (1998); Kd98, Karachentsev & Drozdovsky (1998); KKD00, Karachentsev et al. (2000b); KM96, Karachentsev & Musella (1996); KMa96, Karachentsev & Makarov (1996); KSD01b, Karachentsev et al. (2001b); KSH00, Karachentsev, Sharina & Huchtmeier (2000a); KT94, Karachentsev & Tikhonov (1994); L78, Longmore et al. (1978); LB99, Lee & Byun (1999); LT99, Lynds et al. (1999); M99, Minniti et al. (1999); NED, the NASA Extragalactic Database; P94, Piotto et al. (1994); RC3, de Vaucoulerus et al. (1991); S96, Sharina et al. (1996); S97, Sakai et al. (1997); S99, Sakai & Madore (1999); SHG00, Schulte-Ladbeck et al. (2000); SHG01, Schulte-Ladbeck et al. (2001); SM01, Sakai & Madore (2001); So96, Soria et al. (1996); T95, Tolstoy et al. (1995a); TGD00, Tikhonov, Galazutdinova, & Drosdovskii (2000); TS95, Tolstoy et al. (1995b); TSB01, Tosi et al. (2001).

2.3. Results

The various results of the Hubble-tensor calculation are shown in several following tables. Calculations were done for four cases: anisotropic expansion using the whole 98-galaxy sample, anisotropic using the 35 galaxies with more accurate distances, and isotropic using each sample. For reference, some parallel results from the literature are included.

Considering the reflex solar velocity (\mathbf{v}_0 , shown in Table 2) first, taking different samples and treating them different ways leads to a speed varying over a range of 60 km s⁻¹ and a direction changing over a dozen degrees. Comparing these results with other determinations we find a similar variation. That of Karachentsev & Makarov (2001) uses a somewhat larger but overlapping sample of galaxies going out to a similar distance. Yahil, Tammann & Sandage (1977) only used Local Group galaxies, so their result is not necessarily comparable (though it has been used to correct the radial velocities of more distant galaxies by, for example, Schmidt & Boller (1992)). The expected amount of variation, given the data, will be treated quantitatively below.

The results for the Hubble tensor (as well as the isotropic solutions) are displayed in Table 3. The directions U, V and W are those of the eigenvectors, in no specific order (that is, U is not necessarily the closest eigenvector to X, and U in one solution is not necessarily the closest eigenvector to the U in the other).

Given the amount of attention which is to be paid to the deviations from the models, it is important to try to separate the effects of observational errors from real velocities. For the linear relation between distance and radial velocity, deviations from the models are related by

$$\delta v = H \delta r \tag{4}$$

so the variances are

$$\frac{1}{N}\sum_{i}\delta v_{i}^{2} = H^{2}\frac{1}{N}\sum_{i}\delta r_{i}^{2} \tag{5}$$

If we assume that the distance errors are proportional to distance⁸, and that their distribution once the distance is factored out is independent of them,

$$\frac{1}{N} \sum_{i} \delta v_i^2 = H^2 \frac{1}{N} \sum_{i} r_i^2 \delta x_i^2$$

⁸Strictly speaking, distance errors derived from stellar photometry depend in a rather complicated way on the flux from the target stars and standards and thus on the telescopes and exposure times used. In practice, observations are planned and conducted to a given signal-to-noise ratio and yield errors as an almost constant fraction of distance.

Table 2: Solar Veloc	city
----------------------	------

	v		
Solution	$v, \mathrm{km} \mathrm{s}^{-1}$	\mathbf{L}	В
98, isotropic	290	10	45
98, anisotropic	310	352	62
35, isotropic	350	355	44
35, anisotropic	330	350	49
YTS	334	22.1	28.8
KM01	325	10.9	41.3

Note. — The solar velocity relative to external galaxies according to various computations. The columns are: the calculation; magnitude of velocity in km s $^{-1}$; Supergalactic longitude and latitude, in degrees. The four calculations performed in the present paper are listed first, followed by Yahil, Tammann & Sandage (1977) (based only on Local Group galaxies) then Karachentsev & Makarov (2001), the study most closely comparable to the present one.

Table 3: Hubble Tensor Results

Solution rensor Results	σ	H_{ii}	L	В	Λ_{iiii}
98 Galaxies					
H_{uu}	103	83	127	3	3.46
H_{vv}		51	34	46	1.53
H_{ww}		32	40	-44	0.48
isotropic	118	64			
35 Galaxies					
H_{uu}	77	138	346	-65	1.19
H_{vv}		84	104	-12	4.53
H_{ww}		35	19	21	1.02
isotropic	89	70			
Karachentsev & Makarov (2001)	74	82	132	0	
		62	42	0	
		48		90	

Note. — Solutions for the Hubble tensor calculations, plus isotropic solutions and Hubble tensor components calculated by Karachentsev & Makarov (2001). Columns are: the solution (three lines for tensor solutions); rms dispersion, in km s⁻¹; Hubble component value, in km s⁻¹Mpc⁻¹; Supergalactic longitude and latitude in degrees; corresponding (dimensionless) value of the error tensor (whose use is discussed in the text).

$$= H^2 \frac{1}{N} \sum_i r_i^2 \sum_i \delta x^2$$

For the galaxies with higher-quality distances, the quoted errors range from 0.1 to 0.2 magnitudes with an average of slightly under 0.15, giving a distance error of 7.2%. As noted above, the brightest-star errors are not as well known; but taking 0.4 magnitudes as an estimate yields an average distance error of 20%. Putting these into the above formula gives contributions of 67 and 21 km s⁻¹ of distance errors to the total rms velocity dispersion for the brightest-star and better distances, respectively; which leaves 97 km s⁻¹ of real motion in the 98-galaxy isotropic solution, 78 km s⁻¹ in the 98-galaxy anisotropic solution, and 86 and 74 km s⁻¹ for the respective 35-galaxy solutions⁹.

Compared to the differences in solar reflex velocity among the various calculations it is perhaps reassuring to find among the tensor model results a stable, high value of 82-84 km s⁻¹Mpc⁻¹ close to the supergalactic plane and not far from the direction of Virgo. However, there appears to be no agreement in direction among the other eigenvectors and very wide variation in eigenvalues; indeed, in the solution with the most reliable data the Virgo-pointing eigenvector does not correspond to the largest eigenvalue. Clearly, the reliablility of these results must be investigated.

An appropriate way to compare solutions as a whole is the F-ratio test¹⁰. One finds their respective variances (average square of the deviation from the model; here, the square of the velocity dispersions) and the number of degrees of freedom in each, and then calculates the probability that the larger variance could be produced by the model which better fits the data. Essentially, while a model with more parameters will always give a smaller dispersion, one demands that it give a *significantly* smaller dispersion.

For the 98-galaxy sample, the difference is quite significant: the anisotropic solution is a better fit at the 90% level. For the 35-galaxy sample the probability is lower, 77%, but

 $^{^9}$ Radio HI radial-velocity measurements themselves have quoted accuracies of one to a few km s $^{-1}$, negligible for purposes of these calculations. There are a handful of galaxies with much more inaccurate optical radial velocities, but they have no significant effect on this study.

One might try to set up a sort of inverse method to find the various contributions to the overall velocity dispersion. If one assumes that the deviations from the models are made up of an intrinsic part, say σ_a for the anisotropic model and σ_i for the isotropic model, and the part due to distance errors, σ_{35} and σ_{98} , added in quadrature, we can set up four equations in four unknowns to find the true values of each. Unfortunately, the "intrinsic" velocity dispersions are dispersions around different models; different enough that the four equations are inconsistent with each other and have no common solution.

¹⁰See, for example, Hoel (1971), p. 269. Bronshtein & Semendyayev (1998), p. 629 (section 5.2.3.4) also has a useful discussion. In practice calculations were performed using the program Mathematica.

we may still say that anisotropy is a better fit to the data. (The fact that the more reliable data produce the less certain result, though, is troubling, and will be explored below.)

Clearly some parts of the solutions are better known than others. In an attempt to separate the uncertainties of the various parameters we expand the dispersion as a Taylor series about the solution:

$$\sigma^{2} = \sigma_{0}^{2} + \frac{d\sigma^{2}}{d\mathbf{H}} \cdot \delta \mathbf{H} + \frac{1}{2} \delta \mathbf{H} \cdot \frac{d^{2} \sigma^{2}}{d\mathbf{H}^{2}} \cdot \delta \mathbf{H}$$
 (6)

At the solution the linear term vanishes, and since the variance itself is quadratic in **H** all higher derivatives are identically zero (see equation 3). Restricting ourselves to the quadratic term and shifting to summation by repeated indices,

$$\Delta \sigma^2 = \frac{1}{2} \frac{\partial^2 \sigma^2}{\partial H_{ij} \partial H_{kl}} \Delta H_{ij} \Delta H_{kl} \tag{7}$$

We seek a parameter which is dimensionless and thus more easily compared between different situations. The most obvious is the fractional change in dispersion divided by the fractional change in Hubble tensor, giving a fourth-order tensor:

$$\Lambda_{ijkl} \equiv \frac{\Delta \sigma^2 / \sigma^2}{\Delta H_{ij} \Delta H_{kl} / H_{ij} H_{kl}}
= \frac{1}{2} \frac{\Delta H_{ij} \Delta H_{kl}}{\sigma^2} \frac{\partial^2 \sigma^2}{\partial H_{ij} \partial H_{kl}}$$
(8)

The components of this tensor are conveniently computed from the data:

$$\Lambda_{ijkl} = \frac{H_{ij}H_{kl}}{N\sigma^2} \sum_{r} \frac{x_i x_j x_k x_l}{r^2} \tag{9}$$

where x_i is the coordinate of a galaxy in the *i* direction and *r* its (total) distance. The first fraction shows that a component of this error-tensor is larger as the ratio of eigenvalues to dispersion is larger, and the sum shows the leverage of more distant data points in the particular spatial directions. That is, an eigenvalue of the error-tensor will be larger and the corresponding eigenvalue of the Hubble tensor will be more certain as the Hubble component is larger compared with the variance, and as the data in the direction of the Hubble component are more distant.

As Lynden-Bell et al. (1988) note with their similar construction, a tensor of this sort is difficult to display or interpret in its entirety. However, we only need the values corresponding to specific eigenvalues of specific solutions. The Λ_{uuu} , Λ_{vvvv} and Λ_{www} components, corresponding to the second-order change in the variance for each of the eigenvalues of the two anisotropic solutions, are given in Table 3.

We continue with the F-ratio test as a way of interpreting these components. Recall that a change in the ratio of variance by a certain amount corresponds to a certain probability that one solution is significantly different from another. For the number of degrees of freedom in the 35-galaxy sample, for instance, a ratio of 1.8 means a 95% probability that the smaller variance corresponds to the better solution. The allowable change in the eigenvalue to remain within this 95% window is thus

$$\frac{\Delta H_{ii}}{H_{ii}} = \sqrt{\frac{1.8 - 1}{\Lambda_{iiii}}} \tag{10}$$

The results of this kind of calculation are shown in Table 4.

From the table, the uncertainty in the out-of-plane tensor components is rather large. If 70% confidence is required, for instance, the H_{ww} eigenvalues in each solution are still only known with a 50% error. The effect of these uncertainties on the whole solution may be illustrated by the 35-galaxy H_{uu} eigenvalue. At 70% confidence it may vary by a fraction of 0.44, which means it could have a value of 61 km s⁻¹ Mpc⁻¹, smaller indeed than the middle eigenvalue. In that case its direction ceases to be an eigenvector. As suggested by the great differences in direction and magnitude among the models, the details of anisotropic flow are quite uncertain.

An exactly similar derivation gives the error tensor corresponding to solar reflex motion:

$$\Lambda_{ij} \equiv \frac{\Delta \sigma^2 / \sigma^2}{\Delta V_i \Delta V_j / V_i V_j}$$
$$= \frac{V_i V_j}{N \sigma^2} \sum_n \frac{x_i x_j}{r^2}$$

and in the same way (using the F-ratio test) it can be turned into uncertainties of components of the reflex motion vector. To allow comparison with the entries in Table 2, the 70%-confidence limits of each component (corresponding to about one-sigma error bars) were combined into limits on the magnitude and direction and listed in Table 5. Some of the uncertainty comes from distance errors, which translate into correlated errors in the components; most is uncorrelated. Figures are given for both extremes, with the actual situation being closer to the uncorrelated ideal. For large values of angle uncertainties (about 15° or over) the limits become strongly asymetrical; the figures listed are averages.

For comparison, Karachentsev & Makarov (2001) give their uncertainties (standard errors) as \pm 11 km s⁻¹ in reflex velocity magnitude and one or two degrees in direction; and 3-5 km s⁻¹ Mpc⁻¹ in Hubble tensor components.

Table 4: Uncertainty in Tensor Components

Component	$\Delta H/H, 90\%$	$\Delta H/H,~80\%$	$\Delta H/H, 70\%$
$98 H_{uu}$	0.30	0.23	0.19
$98 H_{vv}$	0.46	0.35	0.28
$98 H_{ww}$	0.82	0.63	0.50
$35 H_{uu}$	0.74	0.58	0.44
$35 H_{vv}$	0.38	0.30	0.22
$35 H_{ww}$	0.80	0.63	0.47

Note. — Uncertainty in Hubble Tensor components, calculated by means of the error tensor. For each of the components in the two solutions, the fractional amount it may change before the solution becomes worse (as measured by an increase in the dispersion) at various confidence levels is shown. Thus, for example, the H_{ww} component in the 98-galaxy solution can change by half its value before it is 70% certain that such a change leads to a worse-fitting solution.

Table 5: Uncertainty in the Solar Reflex Velocity

Solution	Magnitude, $km s^{-1}$	SG Longitude	SG Latitude
98 isotropic	$290 \pm 90, 130$	$10 \pm 15, 12$	$45 \pm 24, 23$
98 anisotropic	$310 \pm 90, 110$	$352 \pm 19, 23$	$62 \pm 13, 4$
35 isotropic	$350 \pm 80, 120$	$355 \pm 6, 7$	$44 \pm 26, 30$
35 anisotropic	$330 \pm 80, 110$	$350 \pm 14, 16$	$49 \pm 24, 26$

Note. — Uncertainty in the Solar Reflex Velocity, calculated by means of the error tensor. The value for each component (magnitude, Supergalactic Longitude, Supergalactic Latitude) is followed by two numbers: the first corresponds to the case of completely uncorrelated errors among the Cartesian vector components, the second to completely correlated errors. The actual situation is closer to the uncorrelated case. Large values for errors in angle are not precise, since nonlinear effects become important for figures larger than about 15°.

2.4. Uncertainty of the Uncertainties

We have at hand three different ways of estimating the uncertainty in our numbers: the variation in parameters between calculations; the formal standard error; and the error tensor. Unfortunately, they do not agree.

Considering the solar reflex velocity (magnitude and direction) and out-of-plane Hubble tensor eigenvectors and eigenvalues, variations between the calculations are much larger than the standard error allows. They are, however, consistent with estimates based on the error tensor. The standard error assumes a rather strict Gaussian distribution of deviations from the model, and that the sample at hand is an unbiased description of it. The error tensor also assumes a Gaussian distribution, but is less strict, in that it takes into account just how the variance changes with this particular data set when changing a parameter. We must conclude, then, that the data at hand do not satisfy the necessary conditions for the standard error: an unbiased sample of an underlying model, with a strictly Gaussian distribution of errors around it. Exactly how the samples fail is not clear from calculations to this point, but two general areas are identifiable.

First, the samples could be chosen with some bias which prevents a good representation of the kinematics of the Local Volume. A good fit to the data may then translate to a poor fit to the real kinematics. This is indicated by the fact that some parameters show a very strong dependence on the particular data set used, and that in places where the data sets overlap (such as in the direction of the 82-84 km s⁻¹ $\rm Mpc^{-1}$ Hubble tensor component) the results are more similar than the error tensor indicates they should be.

Second, the assumed kinematic models could be inappropriate, in that there are systematic motions not considered. This would make the peculiar velocity distribution about the models non-Gaussian. Deviations which are systematic in space will be investigated in the next section, followed by other possibilities.

3. Spatial Deviations from the Hubble Models

In Figures 1 through 12 are plotted the deviations of each galaxy from the various solutions (that is, how much its radial velocity differs from what the model would predict) against the various spatial coordinates. The first figures use Supergalactic X, Y and Z; the second half use U, V and W, constructed along the eigenvectors of the tensor solutions (note that the directions of each U, V and W axis are different in the 98-galaxy and 35-galaxy solutions).

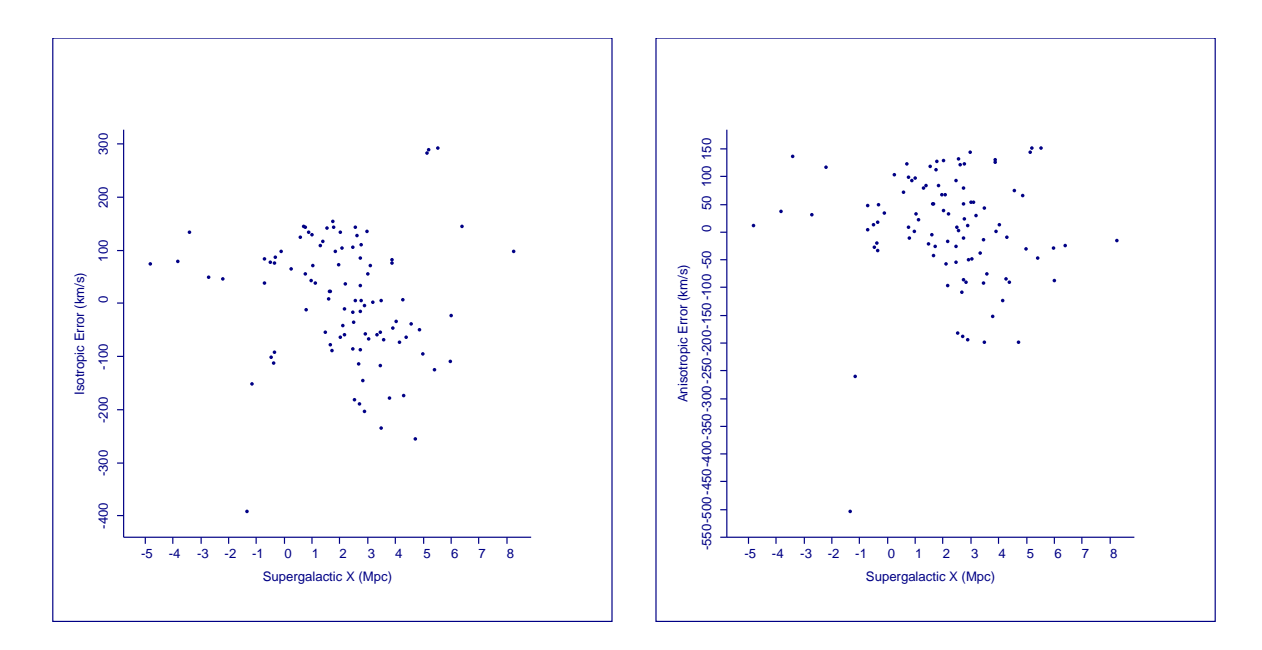


Fig. 1.— Dispersions around the solution against Supergalactic X for the 98 galaxy isotropic (left) and tensor (right) solutions.

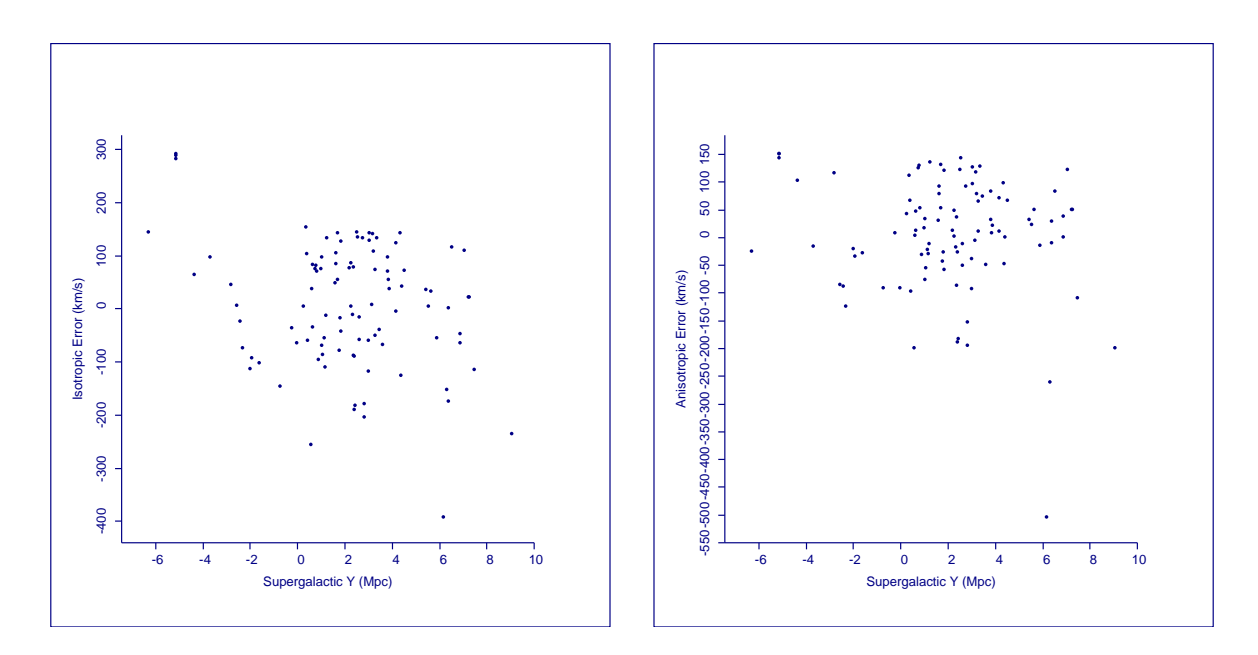


Fig. 2.— Dispersions around the solution against Supergalactic Y for the 98 galaxy isotropic (left) and tensor (right) solutions.

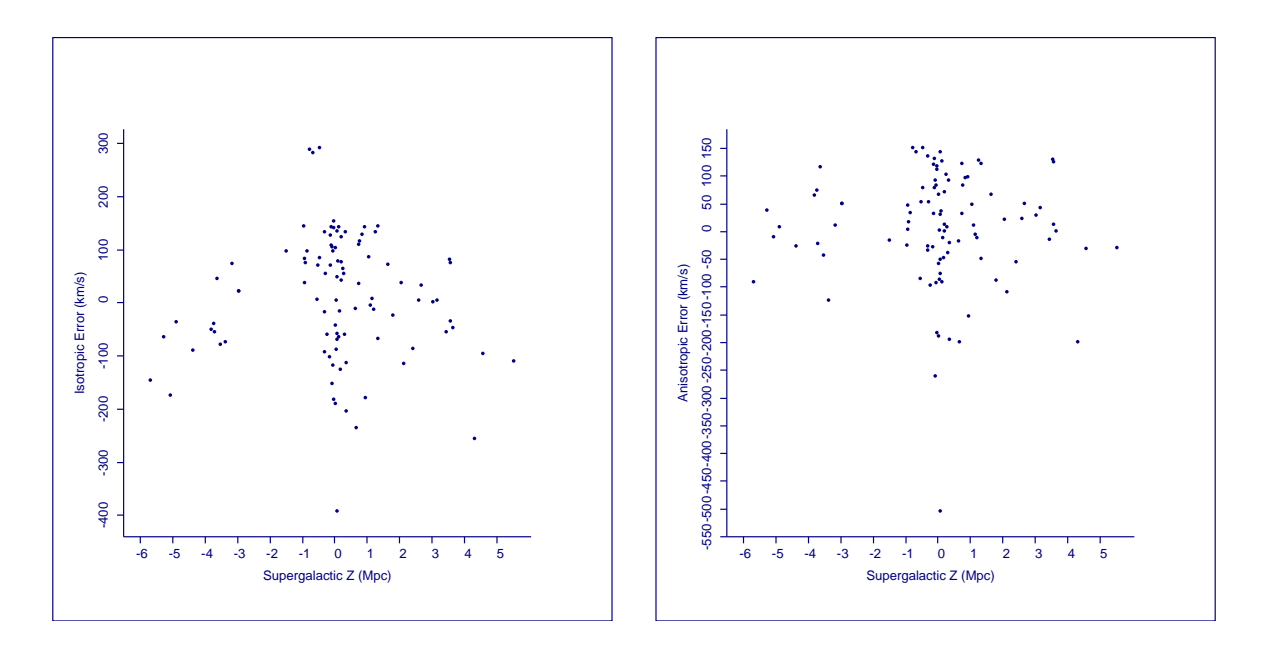


Fig. 3.— Dispersions around the solution against Supergalactic Z for the 98 galaxy isotropic (left) and tensor (right) solutions.

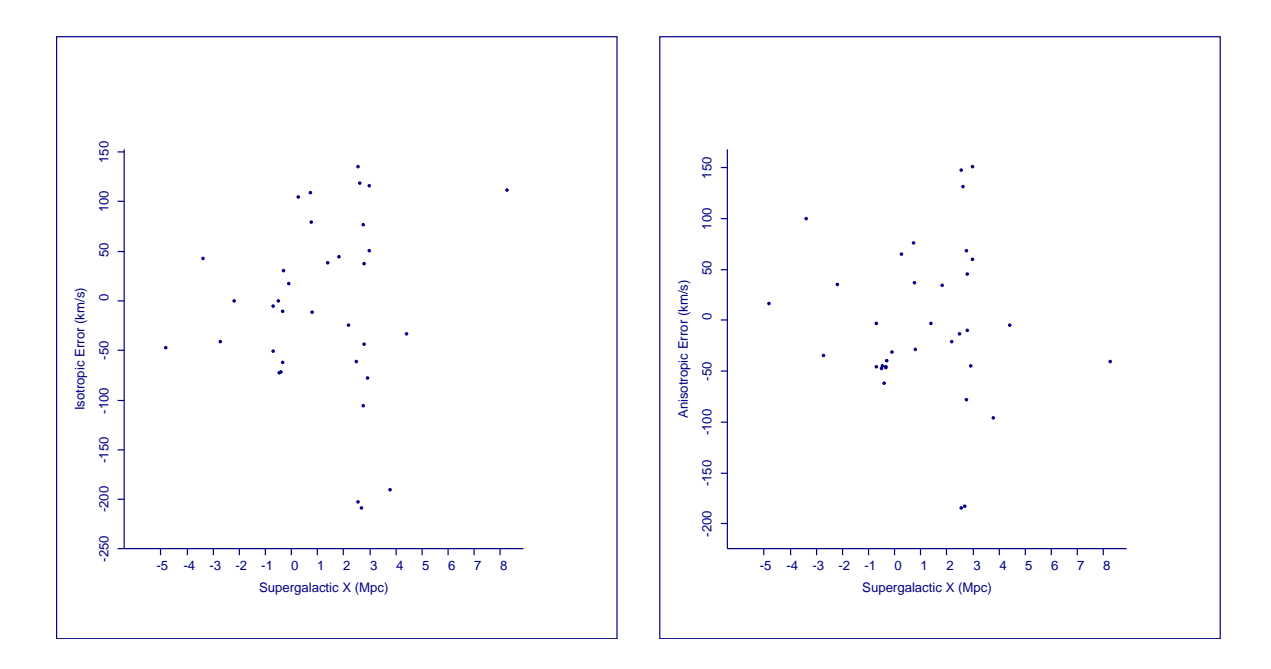


Fig. 4.— Dispersions around the solution against Supergalactic X for the 35 galaxy isotropic (left) and tensor (right) solutions.

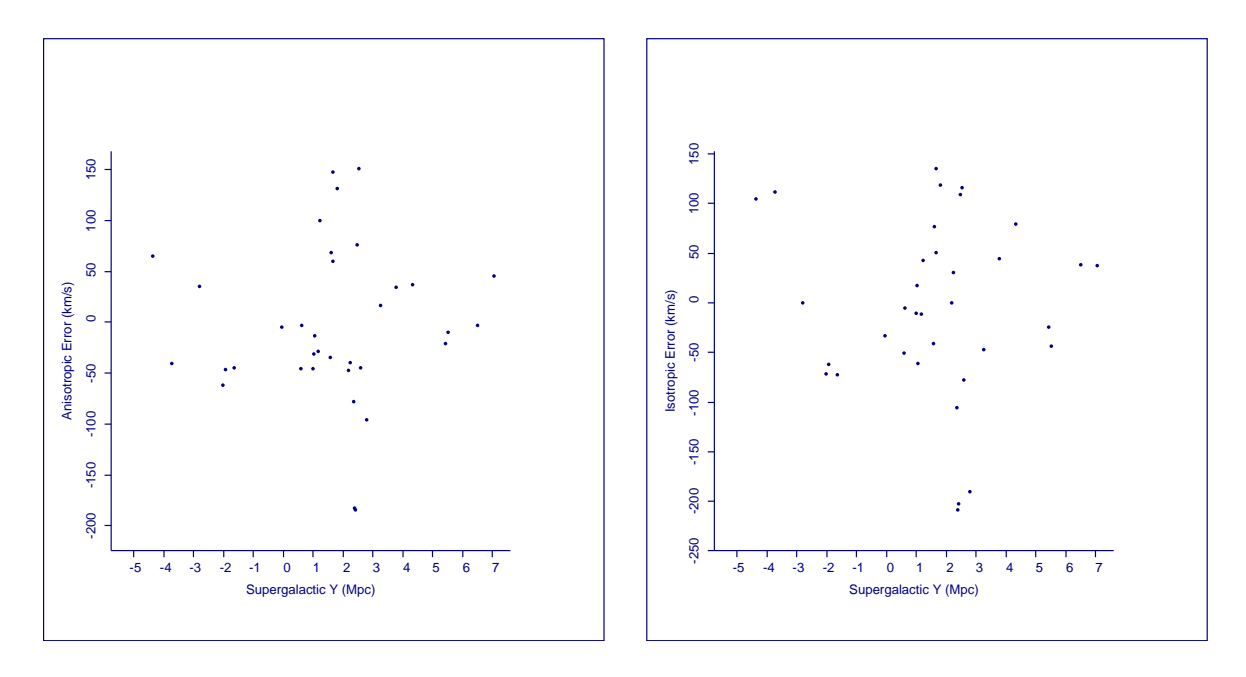


Fig. 5.— Dispersions around the solution against Supergalactic Y for the 35 galaxy isotropic (left) and tensor (right) solutions.

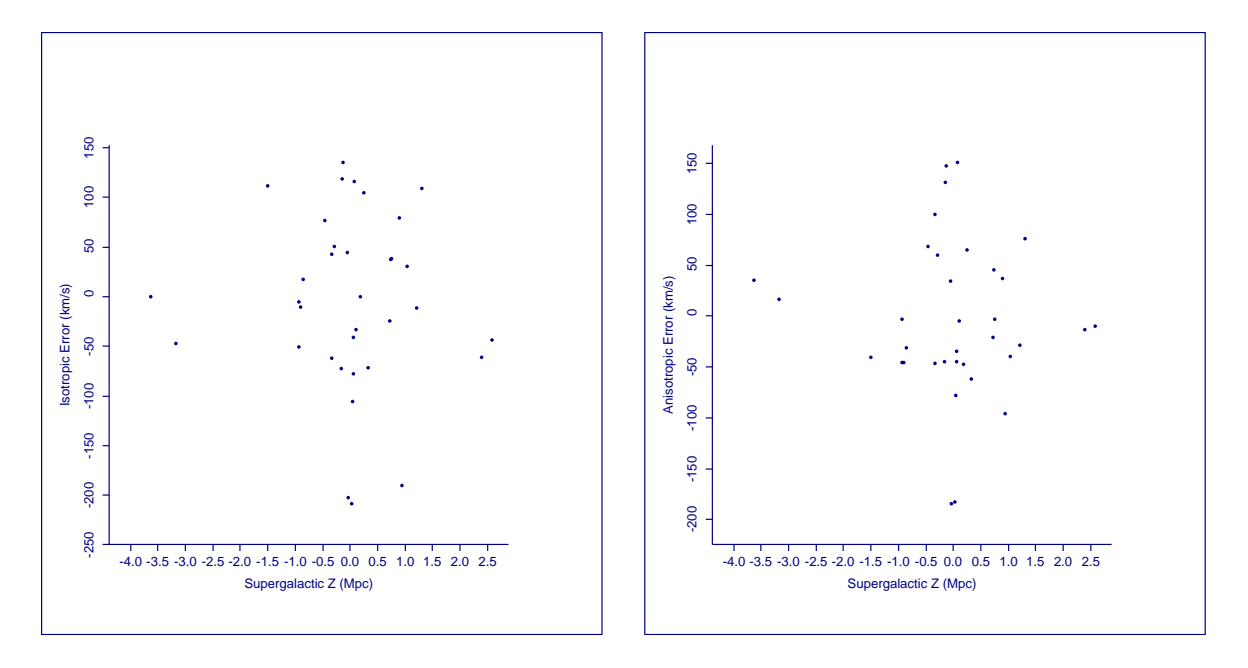


Fig. 6.— Dispersions around the solution against Supergalactic Z for the 35 galaxy isotropic (left) and tensor (right) solutions.

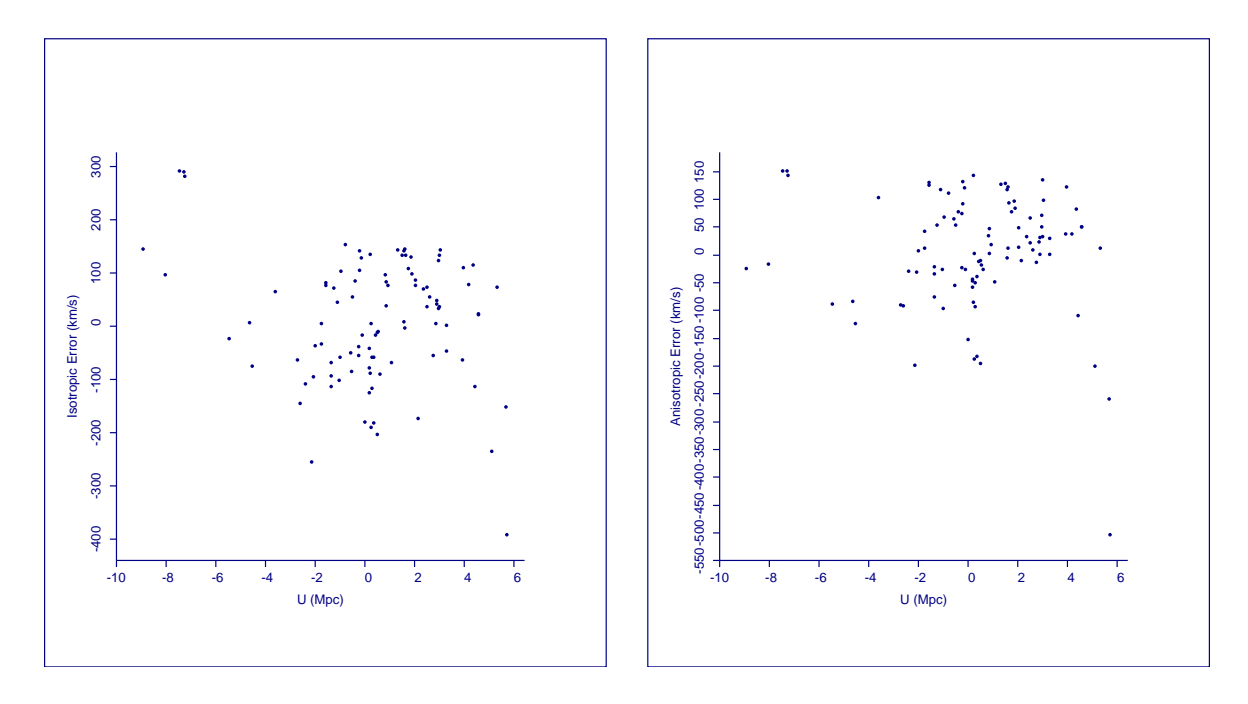


Fig. 7.— Dispersions around the solution against eigenvector U ($L = 127^{\circ}$, $B = 3^{\circ}$) for the 98 galaxy isotropic (left) and tensor (right) solutions.

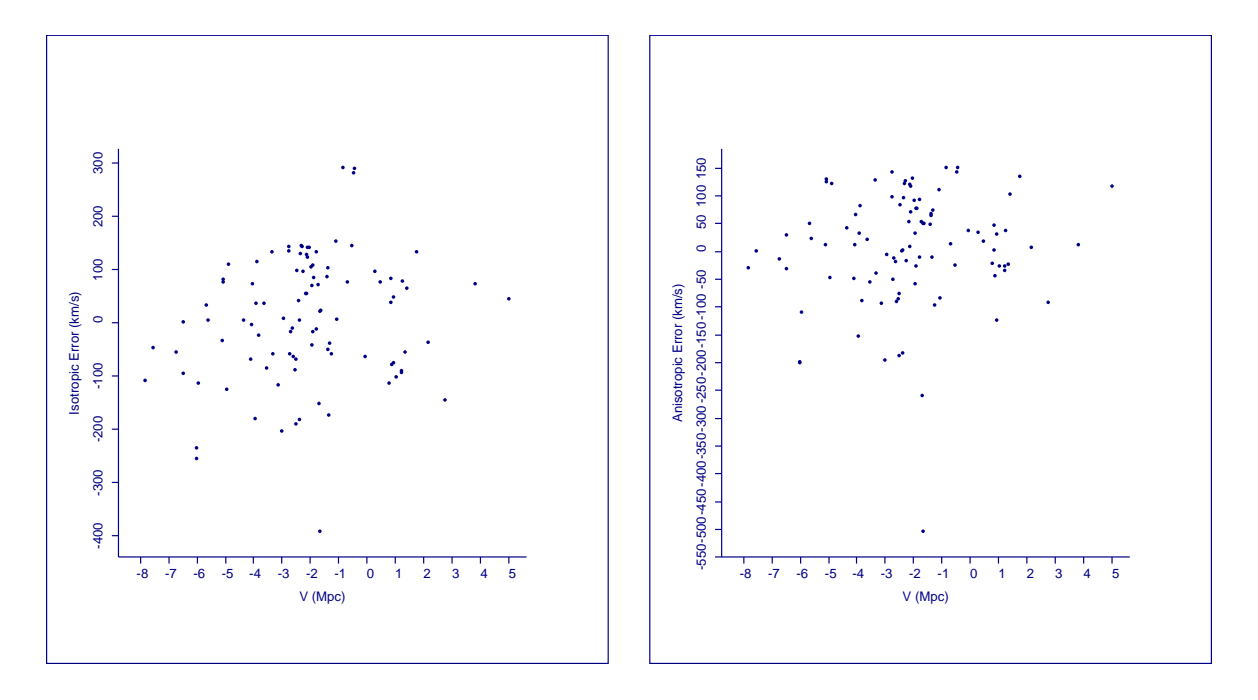


Fig. 8.— Dispersions around the solution against eigenvector V ($L=34^{\circ}$, $B=46^{\circ}$ for the 98 galaxy isotropic (left) and tensor (right) solutions.

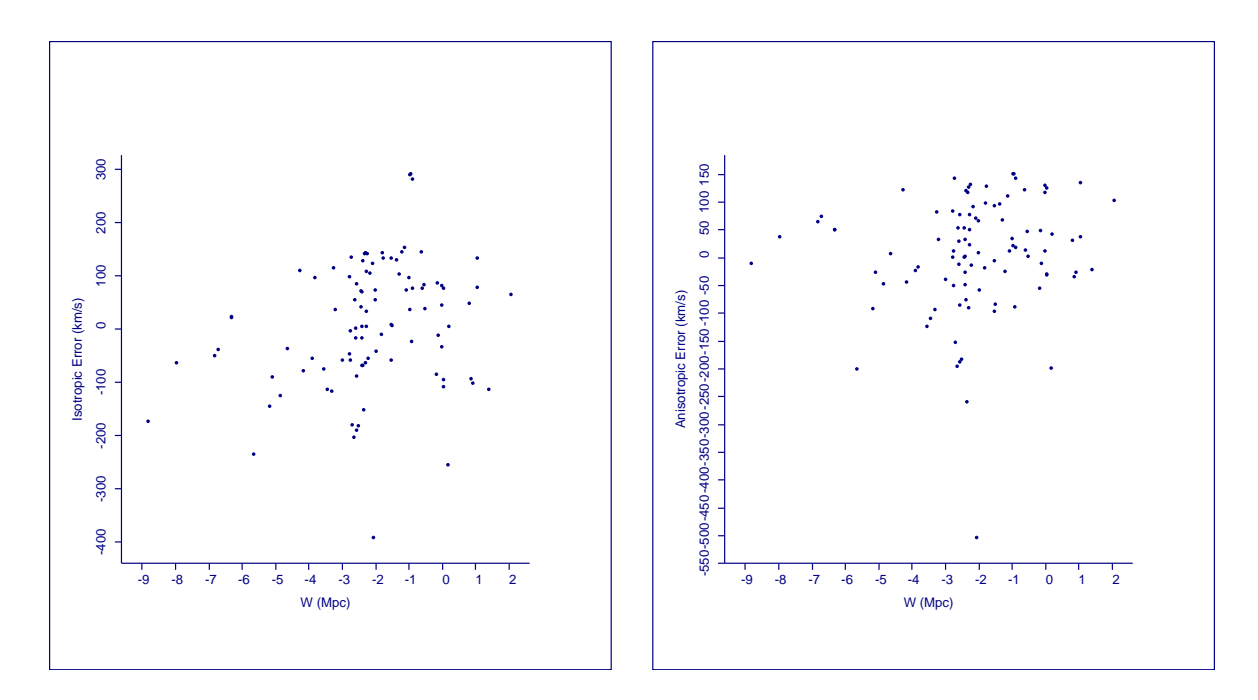


Fig. 9.— Dispersions around the solution against eigenvector W (L = 40° , B = -44°) for the 98 galaxy isotropic (left) and tensor (right) solutions.

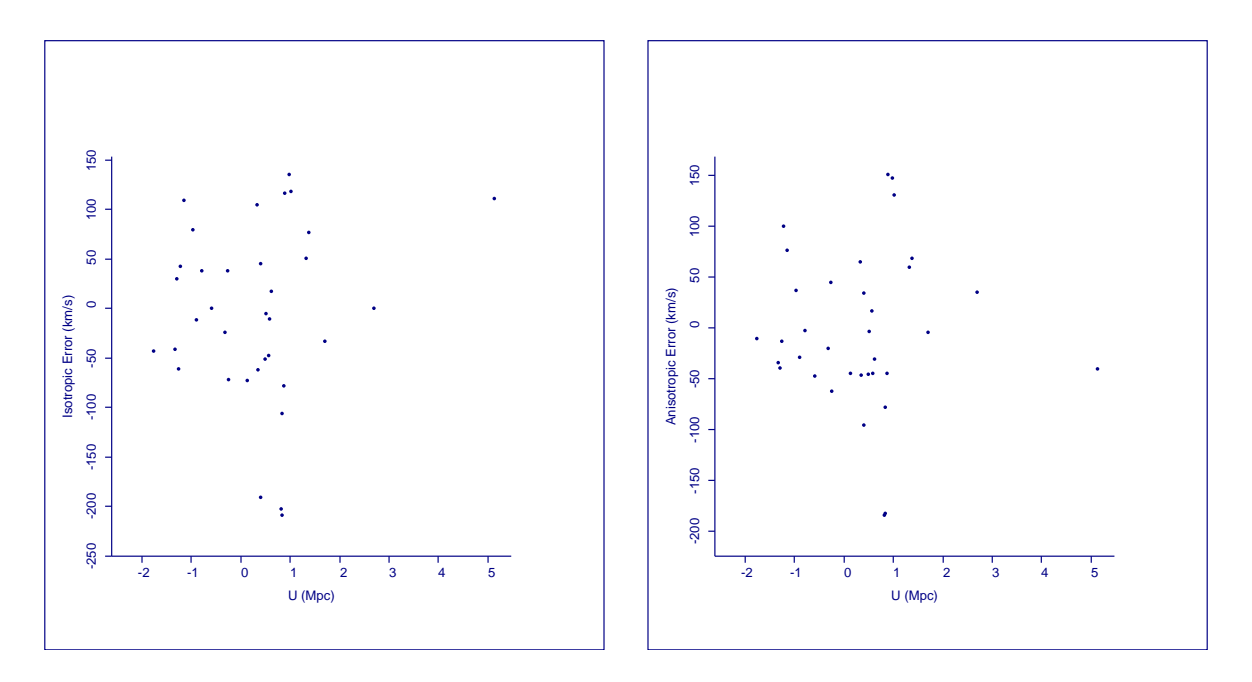


Fig. 10.— Dispersions around the solution against eigenvector U ($L=66^{\circ}$, $B=65^{\circ}$) for the 35 galaxy isotropic (left) and tensor (right) solutions.

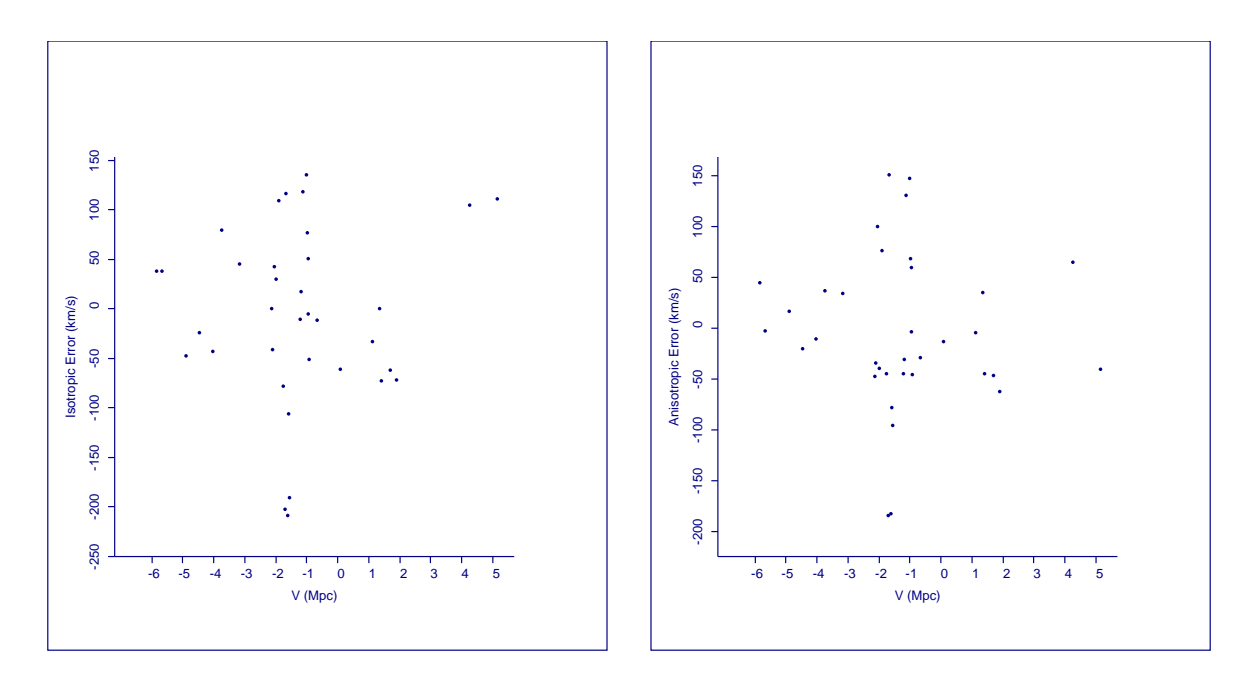


Fig. 11.— Dispersions around the solution against eigenvector V (L = 104° , B = -12°) for the 35 galaxy isotropic (left) and tensor (right) solutions.

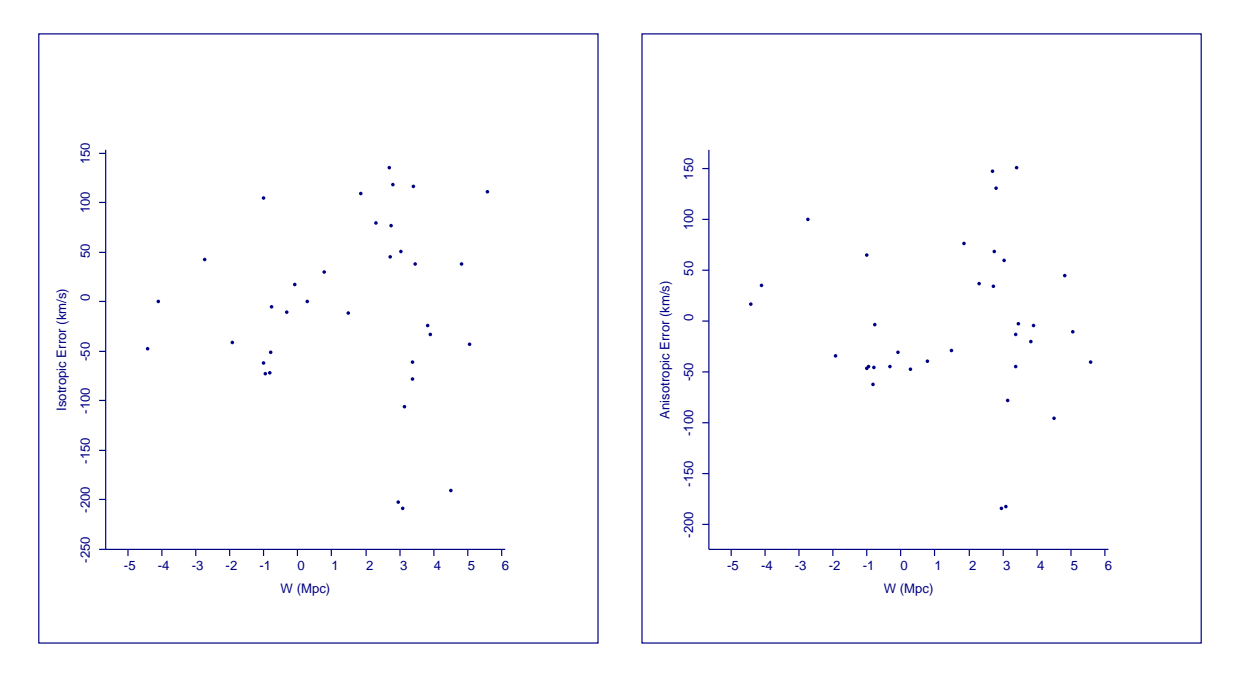


Fig. 12.— Dispersions around the solution against eigenvector W ($L=19^{\circ}, B=21^{\circ}$) for the 35 galaxy isotropic (left) and tensor (right) solutions.

The most important point about these plots is the *lack* of any pattern. The deviation of any particular galaxy from a model appears to be quite random in space (with exceptions to be pointed out).

Consider in detail, for example, the Supergalactic X plots. There is clearly a lack of galaxies at negative X values, reflecting the uneven distribution of data. There is no clear trend of error with postion, though the total width of the error is reduced somewhat in the anisotropic solution. The isolated point with a -400 to -500 km/sec⁻¹ error is UGC 7857, a dwarf galaxy with only a brightest-star distance, in the general direction of the Virgo cluster. The distance may be in error, or the redshift could be affected by a superimposed star (a problem noted several times in Whiting, Hau & Irwin (2002)); or, just possibly, it could represent a very high-velocity tail of the peculiar velocity distribution (a matter discussed below). Note also that, in areas with points, the density is approximately constant. That is, there is no apparent concentration around any given value. This important observation will be expanded below.

The 98-galaxy Supergalactic Z, isotropic plot does show interesting systematic behavior. Recall that these are the residual radial velocities after the average expansion of the cloud of galaxies has been subtracted. There appears to be a trend for galaxies with Z < -2 to line up from lower left to upper right, which would indicate a lower effective Hubble constant normal to the Supergalactic Plane. This was noted by Karachentsev & Makarov (1996) in their similar plot. This flow is easily interpreted as the expected lower effective Hubble constant normal to the Plane.

However, it disappears in the plot of higher-quality data (in part, it must be noted, because the high-quality coverage of high-latitude galaxies is poor). More important, it does not show up in the Hubble tensor calculation in the form of a low eigenvalue in the direction of the Supergalactic Pole, the nearest eigenvector being 45° away. It is not, then, a sign of any average slower Hubble flow out of the Plane.

Going to the coordinate system defined by the eigenvectors of the calculated tensors, first we note that the 98-galaxy U plots look much like the Supergalactic Y plots. This is no surprise, since the respective axes are only a few degrees apart. There is no clear trend in the other plots. In particular, the dynamical behavior discerned above in the 98-galaxy, Supergalactic Z plot (Figure 3) has faded or disappeared. The fact that the calculated eigenvectors might actually conceal information on the kinematics of the system is an indication that they are not useful in its description. This reinforces the conclusion of the previous section: the anisotropic flow models tell more about a given data set than about the underlying galaxy motions.

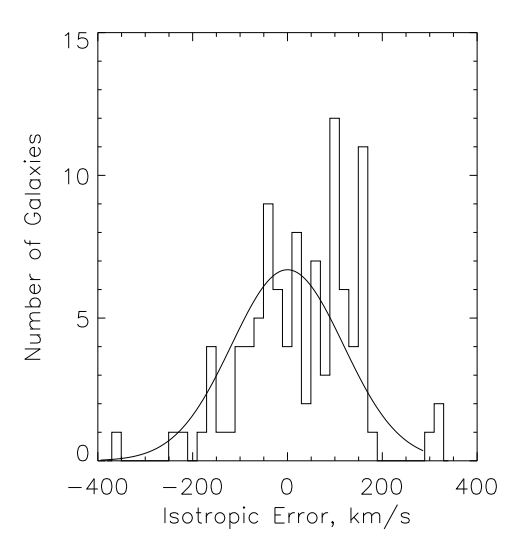
The overall lack of any systematic behavior in the spatial plots is very significant. It means that, at least as far as these data can show, there are no significant "bulk flows" within the 10 Mpc volume. Also, any nonlinear effects, such as a second-order tidal effect from the Virgo cluster, would show as a curve in at least some of the plots; none are there. In addition, significant mass concentrations should result in a localized increase in the peculiar velocity width; nothing of this kind is seen, although the data are too sparse to rule it out entirely.

4. The Peculiar Velocity Distribution

4.1. The Shape of the Velocity Distribution

It has been noted that there was no obvious concentration of deviations from each model near zero; that is, it was roughly as likely to find galaxies far from the model as close to it. This is made more quantitative by Figures 13 and 14, which show histograms of the number of galaxies against the deviation from model flows¹¹. In each case a Gaussian distribution with the same average and standard deviation has been superimposed.

 $^{^{11}}$ Only the 98-galaxy solutions are shown, since 35 galaxies do not provide enough information to produce a useful histogram. The choice of bin sizes is a compromise between having enough galaxies in each bin to be significant, and having enough bins to show a shape. The 20 km s⁻¹ bins are clearly rather noisy, so 40 km s^{-1} bins are shown for comparison. Between them, any spurious signals due to unfortunate binning should be eliminated.



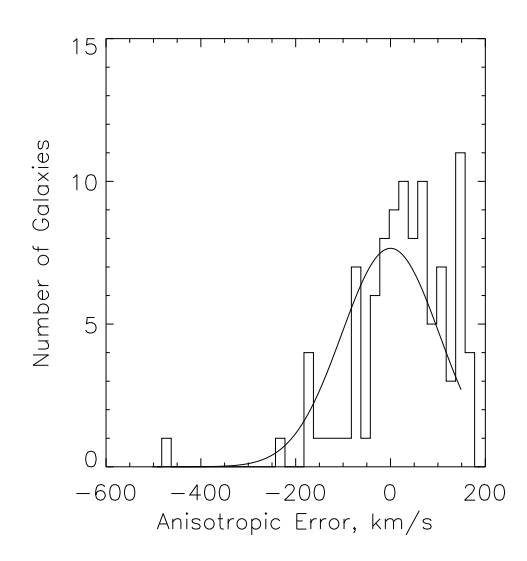
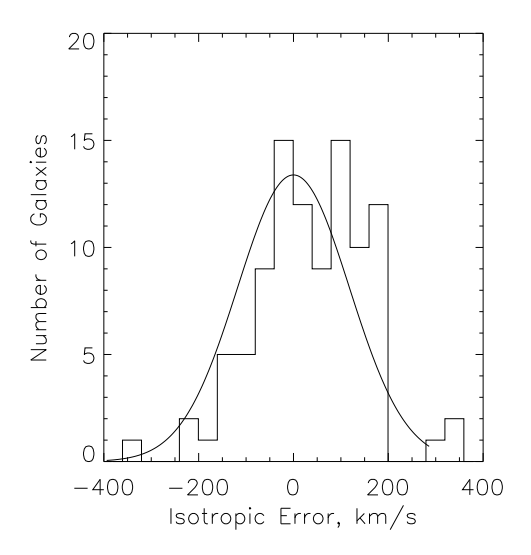


Fig. 13.— Histogram of velocity errors about the isotropic (left) and tensor (right) solutions for 98 galaxies. Bins are 20 km sec⁻¹ wide. Gaussian distributions of the same rms width, average, and normalization are shown superimposed.



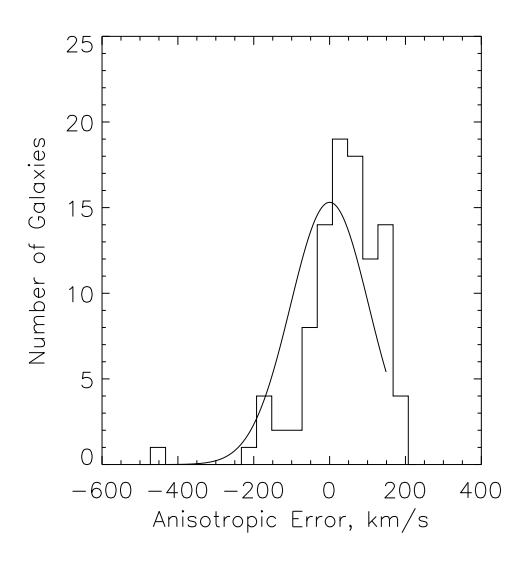


Fig. 14.— Histogram of velocity errors about the isotropic (left) and tensor (right) solutions for 98 galaxies. Bins are 40 km sec⁻¹ wide. As before, corresponding Gaussian distributions are also shown.

Each histogram is markedly asymmetric, showing a clear slope upward toward positive errors and a rather abrupt cutoff. (Quantitatively, a χ -squared test comparing the four histograms to Gaussian distributions enables us to rule them out with 98% to over 99% confidence.) This is almost certainly a selection effect. When making up a list of galaxies out to a certain distance, those with high radial velocities are generally excluded, the assumption being that most of that velocity is due to Hubble flow (for instance, Schmidt & Boller (1992)). Those with a peculiar velocity slightly larger than 200 km sec⁻¹ in addition to a Hubble flow of 300 km sec⁻¹ (appropriate to 5 Mpc at the average local Hubble value from the calculations here) simply will not be included in a sample limited to 500 km sec⁻¹. While the galaxies in the present data samples are known from information other than radial velocities to be close by, one may expect most of them (at least) to have been chosen for study initially based on radial velocity.

The lack of high radial velocity galaxies in the sample means that the Hubble constant and Hubble tensor eigenvalues calculated above are biased low. The velocity dispersion given in Table 3 for each solution is also significantly underestimated, and there must be many known galaxies not now considered members of the Local Volume which in fact reside there. (This statement probably does not apply to the brightest and most important galaxies in the sky, which have been well-studied and which have other sorts of distance estimates. But there should be many of middling brightness and importance which are much closer than has been assumed, and certainly many dwarfs.) In addition, statistical estimators based on Gaussian statistics can no longer be trusted; this reinforces the results in section 2.4.

Unfortunately, the actual values cannot be estimated from the data without a good idea of the quantitative form of the selection effect, and the quality and quantity of information at hand simply do not allow us to derive it. Formally, one might have an almost unlimited peculiar velocity distribution, as long as it is balanced by a high Hubble constant to avoid a large population of galaxies with negative radial velocities (which would certainly have been noticed, but haven't been observed).

One might try to fit the observed shape of a histogram to an assumed form of the peculiar velocity distribution, either Gaussian (which assumes a dynamically young system), Maxwellian (which assumes a dynamically old system) or the more sophisticated function derived by Saslaw et al. (1990), assuming that the low-radial velocity end of the distribution is accurate. However, note that if error bars of \sqrt{n} are added to each bin in Figure 14 (isotropic model), that is if Poisson statistics are assumed, the shape is consistent with a flat distribution from -150 to +200 km s⁻¹; a monotonic linear increase from -250 to +200 km s⁻¹, abruptly cut off at the upper limit; a Gaussian with a center about +50 km s⁻¹ and its high-velocity end truncated; or a Maxwellian similarly biased and truncated. The data at

hand simply do not allow accurate curve fitting¹².

If we guess that the distributions shown actually contain most of the peculiar velocity dispersion (alternatively, that the Hubble constant is not biased very much), then 200 km s⁻¹ forms a rough limit to the observed dispersion and the rms value is something over half that¹³. A substantially unbiased sample must then include radial velocities out to about 700 km \sec^{-1} for 5 Mpc and 1000 km \sec^{-1} for 10 Mpc.

4.2. Mass, Light and the Coldness of the Local Flow

Using a sample of nine galaxies extending to about 8 Mpc, Sandage (1986) concluded that the velocity field in the Local Volume was extremely quiet, the velocity dispersion being about equal to the observational errors in distance, near 60 km sec⁻¹. Ekholm et al. (2001) repeated the calculation with 14 galaxies having Cepheid distances, obtaining a similar dispersion of 40-60 km sec⁻¹. A flow this cold is difficult to explain theoretically, recent attempts including those of Baryshev, Chernin, & Teerikorpi (2001) and Axenides & Perivolaropoulos (2002). However, the fact of a cold flow has been disputed, by de Vaucouleurs & Bollinger (1979) for instance, and the present study indicates a dispersion twice that of Ekholm et al. (2001) even ignoring the sample incompleteness at high radial velocity. In any investigation of kinematics in the Local Volume this disagreement requires some explanation.

The non-Local Group galaxies used by Ekholm et al. (2001) in their study are shown in Figure 15, as they fall in the 35-galaxy anisotropic solution. They clearly do not explore the full width of the velocity dispersion. This is easily explained if the Cepheid galaxies are more massive than the average, and thus harder to disturb by gravitational interaction (and a priori plausible, given that Cepheids are easier to find in massive spirals). However, in the right hand side of the same figure several galaxies are singled out which are about as massive as the Cepheid set, perhaps more so, and show a much greater dispersion. It appears that the various cold-flow groups have been misled by small number statistics¹⁴.

 $^{^{12}}$ A χ -squared fit on a flat distribution shows it to be overall a worse fit than the superimposed Gaussians. However, the linear "sawtooth" mentioned above is much better, being rejected at only the 82% level. It is not offered seriously as a model, but shows how asymmetric the distribution really is.

¹³These figures include, of course, a dispersion from observational errors in distances.

 $^{^{14}}$ However, on much larger scales, where motions of the order of 600 km sec⁻¹ are found, a dispersion of 100-200 km sec⁻¹ is still cold. In this context the cold-flow problem remains, though it changes character and may not be as intractable theoretically (see, for instance, van de Weygaert & Hoffman (2000)).

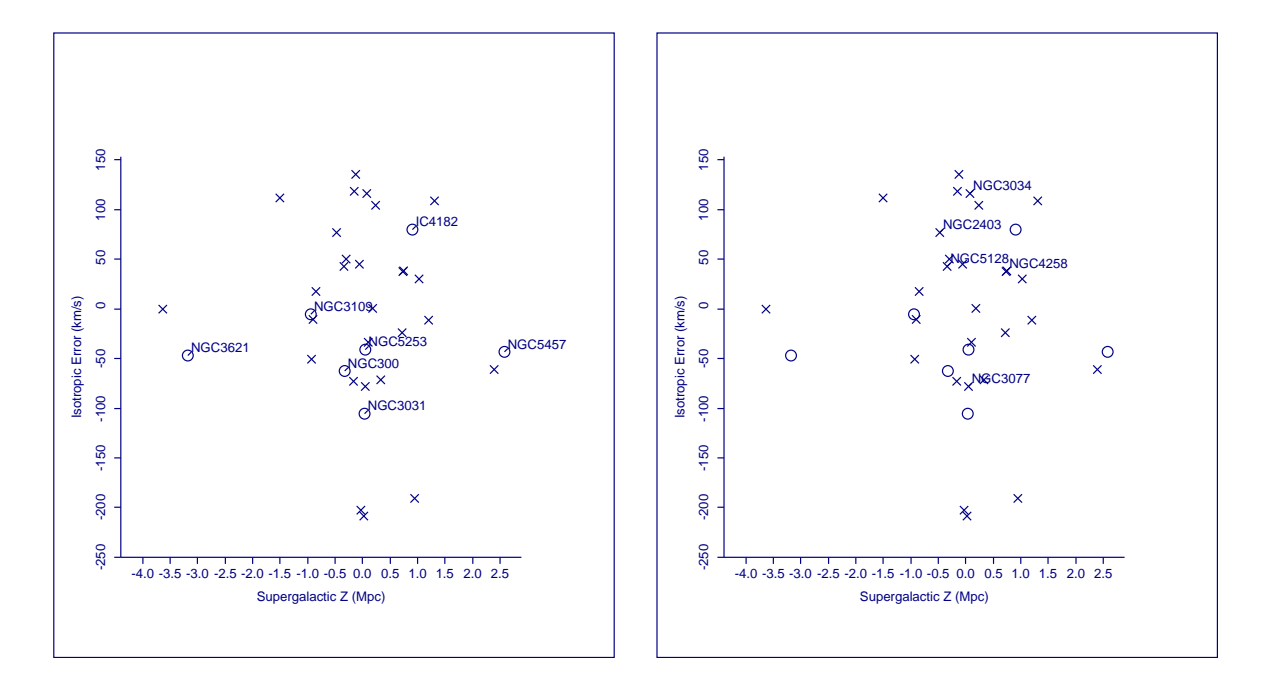


Fig. 15.— Left, non-Local Group galaxies used by Ekholm et al. (2001) to derive a cold local flow are named as they appear on the plot of the 35-galaxy solution. Right, some of the more massive galaxies not used in their investigation on the same plot.

But this raises a very important point. We still expect that, if peculiar velocities are generated by (two- or few-body) gravitational interaction among galaxies, more massive galaxies should have smaller peculiar velocities. Figure 15 suggests it might not be true; in addition, Karachentsev & Makarov (2001) reported no difference in dispersion between group and field galaxies, and between giant and dwarf galaxies. It is a matter worth investigating in some detail.

Reliable, or even consistent, dynamical estimates of galaxy masses are even harder to perform (and thus rarer) than distance measurements. As a surrogate we will use total brightness, assuming some sort of relation between mass and light to be made more specific later. Apparent B magnitudes and extinction estimates from NED (the Schlegel, Finkbeiner & Davis (1998) extinction figures) were combined with distances to produce corrected absolute magnitudes for 97 of the 98 galaxies in the sample¹⁵. Morphological types were also extracted from NED. Finally, each galaxy was assigned to a group or to the field, mostly following Schmidt & Boller (1992), though further investigation was required for some galaxies not in that paper¹⁶. Apparent magnitude and type have already been listed in Table 1; the derived absolute magnitude, NED extinction, and group assignments are listed in Table 6.

¹⁵UGC 6451 had no listed photometry.

¹⁶The assignment of galaxies to groups or to the field is not an exact process, even when done with more care than has been used here. Whether a galaxy is gravitationally bound to a group depends upon the group's total mass, which is poorly known for even the best-studied groups; and upon distances in three dimensions to all galaxies in the area, which are not known for most of the galaxies in the Local Volume. And even were it possible to determine bound members of all groups, there would still be a population not bound to, but still greatly affected by, a nearby group. For the purpose of detecting gross differences in the two populations, however, the division carried out here should be sufficient.

Table 6. Absolute Magnitude, Extinction and Groups

Designation	Mag	Extinction	Group
A0554+0728	-12.9	2.553	F
Antlia	-9.8	0.342	F
BK3N	-10.5	0.345	B2
DDO13	-15.7	0.276	M74
DDO50	-16.5	0.139	B2
DDO53	-13.1	0.160	B2
DDO63	-16.4	0.207	B2
DDO66	-13.7	0.343	B2
DDO70	-13.9	0.137	F
DDO71	-10.1	0.412	B2
DDO75	-14.0	0.188	F
DDO82	-15.0	0.188	B2
DDO155	-12.2	0.113	F
DDO165	-15.7	0.104	B2
DDO187	-12.7	0.105	F
DDO190	-14.1	0.052	F
ESO294-G10	-10.6	0.024	B7
IC342	-19.9	2.407	B1
IC4182	-15.3	0.059	B5
IC2574	-17.2	0.156	B2
KDG52	-10.9	0.091	B2
KDG61	-12.5	0.309	B2
KDG73	-13.2	0.080	B2
KK251	-13.4	1.238	N6946
KK252	-13.4	1.910	N6946
KKR25	-9.4	0.036	F
KKR55	-14.6	2.941	N6946
KKR56	-14.6	3.135	N6946
KKR59	-16.5	3.863	B2
Maffei1	-21.9	5.046	B1
NGC59	-15.2	0.088	F

Table 6—Continued

Designation	Mag	Extinction	Group
NGC300	-17.6	0.055	В7
NGC628	-19.7	0.301	M74
NGC784	-16.5	0.255	F
NGC925	-19.4	0.326	N1023
NGC1560	-16.5	0.813	B1
NGC1705	-15.8	0.035	F
NGC2366	-16.4	0.157	B2
NGC2403	-18.8	0.172	B2
NGC2683	-19.3	0.142	F
NGC2903	-20.2	0.134	F
NGC2976	-17.8	0.300	B2
NGC3031	-20.3	0.346	B2
NGC3034	-19.3	0.685	B2
NGC3077	-17.6	0.289	B2
NGC3109	-15.5	0.288	F
NGC3274	-16.4	0.104	F
NGC3621	-19.3	0.346	F
NGC4144	-17.9	0.065	B4
NGC4236	-17.6	0.063	B2
NGC4244	-17.5	0.090	B4
NGC4258	-20.4	0.069	F
NGC4395	-17.6	0.074	B4
NGC4449	-17.4	0.083	B4
NGC4523	-14.8	0.166	F
NGC4605	-17.7	0.062	F
NGC5128	-20.5	0.496	B6
NGC5204	-16.4	0.054	В3
NGC5236	-20.4	0.284	B6
NGC5238	-14.7	0.046	В3
NGC5253	-16.9	0.242	B6
NGC5457	-20.9	0.037	В3

Table 6—Continued

Mag	Extinction	Group
-17.9	0.047	В3
-15.1	0.048	В3
-18.6	0.067	В3
-14.3	0.302	F
-21.0	1.475	N6946
-14.2	3.162	F
-13.5	0.331	F
-15.5	0.273	M74
-12.6	0.252	M74
-14.9	1.349	F
-14.4	0.384	F
-14.4	0.253	F
-15.5	0.218	F
-14.7	0.145	F
-13.5	0.122	F
-12.6	0.146	B2
-16.4	0.104	F
-11.9	0.257	B2
-14.1	0.155	F
-15.6	0.045	B4
-13.5	0.110	B4
-14.7	0.113	B4
-13.8	0.060	B4
-14.4	0.103	F
-15.0	0.065	F
-15.0	0.039	F
-13.5	0.064	В3
-12.5	0.051	В3
-13.8	1.319	N6946
-16.8	4.061	B1
-16.3	3.419	B1
	-17.9 -15.1 -18.6 -14.3 -21.0 -14.2 -13.5 -15.5 -12.6 -14.9 -14.4 -15.5 -14.7 -13.5 -12.6 -16.4 -11.9 -14.1 -15.6 -13.5 -14.7 -13.8 -14.4 -15.0 -15.0 -13.5 -12.5 -13.8 -16.8	-17.9

Table 6—Continued

Designation	Mag	Extinction	Group
UGCA105 UGCA281 UGCA290 UGCA438	-15.0 -13.8 -13.2 -12.8	0.065 0.060	B1 B5 B4 B7

Note. — Absolute magnitudes for the galaxies in the sample, derived from NED photometry and extinctions, and the distances listed in Table 1. The extinction estimates are shown, as well as the group assignments mostly following Schmidt & Boller (1992). "F" denotes a field galaxy; M74, belonging to the M74 group; N1023 and N6946 one belonging to the NGC 1023 and NGC 6946 groups, respectively.

The data are plotted in Figures 16 and 17. Deviation from the various flow models is shown as a function of absolute magnitude; in addition, symbols designate morphological classes of galaxies.

These figures represent a very remarkable result. Over a range of ten magnitudes in luminosity there is *no* systematic variation in the peculiar velocity dispersion. Further, there is no apparent variation with galaxy type.

Could these plots actually be dominated by the effects of observational errors, rather than real motions? That would require Cepheid and TRGB distance uncertainties to be something like three times their normally estimated size, which seems unlikely. In addition, a dispersion due solely to distance errors would be Gaussian in shape, which these are not; would require a dispersion which increased with distance, which as Figure 18 shows, is not true¹⁷; and would require that the underlying, physical velocity dispersion be almost zero, a very difficult thing to manage theoretically (as noted above) and hard to believe in the context of a galaxy group.

There is the possibility of errors due to other sources. The photometry found in NED is admittedly hetrogeneous, and measurement of the total light from the diffuse and faint outskirts of a galaxy is notoriously difficult. But a comparison of various photometric measurements in NED (where galaxies have been measured more than once) shows a remarkable agreement, figures seldom diverging by as much as 0.2 magnitude. The exceptions are those visually estimated from photographic plates, which have claimed accuracies of about \pm 0.5 magnitude. Being conservative and allowing points in Figures 16 and 17 to move sideways a full magnitude, and postulating some unknown process which preferentially biased high the photometry for galaxies with high peculiar velocities, the shape of the plots remains.

Extinction is another fruitful source of error. But only two of the points in Figure 17 have as much as half a magnitude of extinction. Though both are outliers, removal still leaves the shape intact.

It appears, then, that the constancy of the peculiar velocity dispersion with absolute magnitude is a real effect. What would we actually expect?

Naively, for any two-body interaction, the velocities of galaxies should be changed in inverse proportion to their masses; for a completely relaxed system, with kinetic energy equally partitioned, the random velocities should be inversely proportional to the square root of the masses. Suppose that the mass-to-light ratio lowers by a factor of 100 between

¹⁷Since the number of galaxies in the sample is roughly constant with distance, clear from the plot, it is a posteriori unnecessary to deal with Malmquist and related biases.

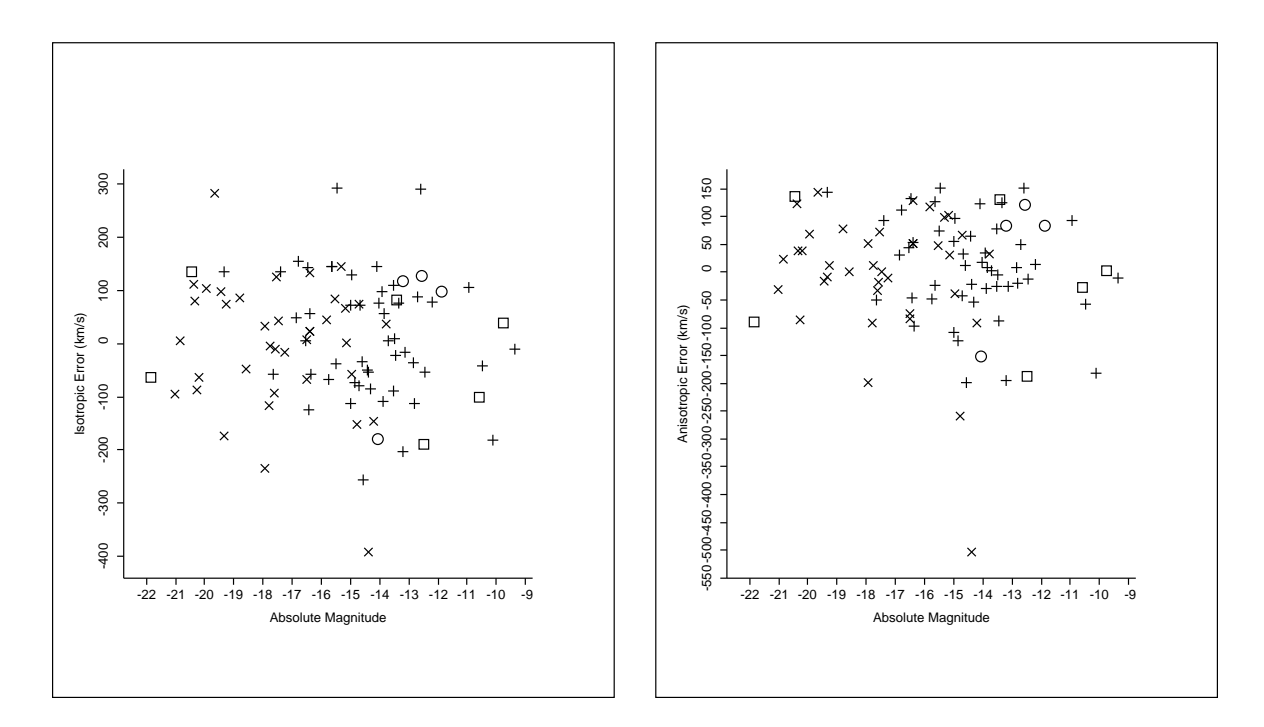


Fig. 16.— Deviation from (left) isotropic and (right) anisotropic Hubble expansion as a function of absolute magnitude for the 97-galaxy sample, using distances, photometry and extinction measurements from the literature. Crosses indicate spiral galaxies; plus, irregular; boxes, elliptical or lenticular; circles, other, peculiar or unclassified.

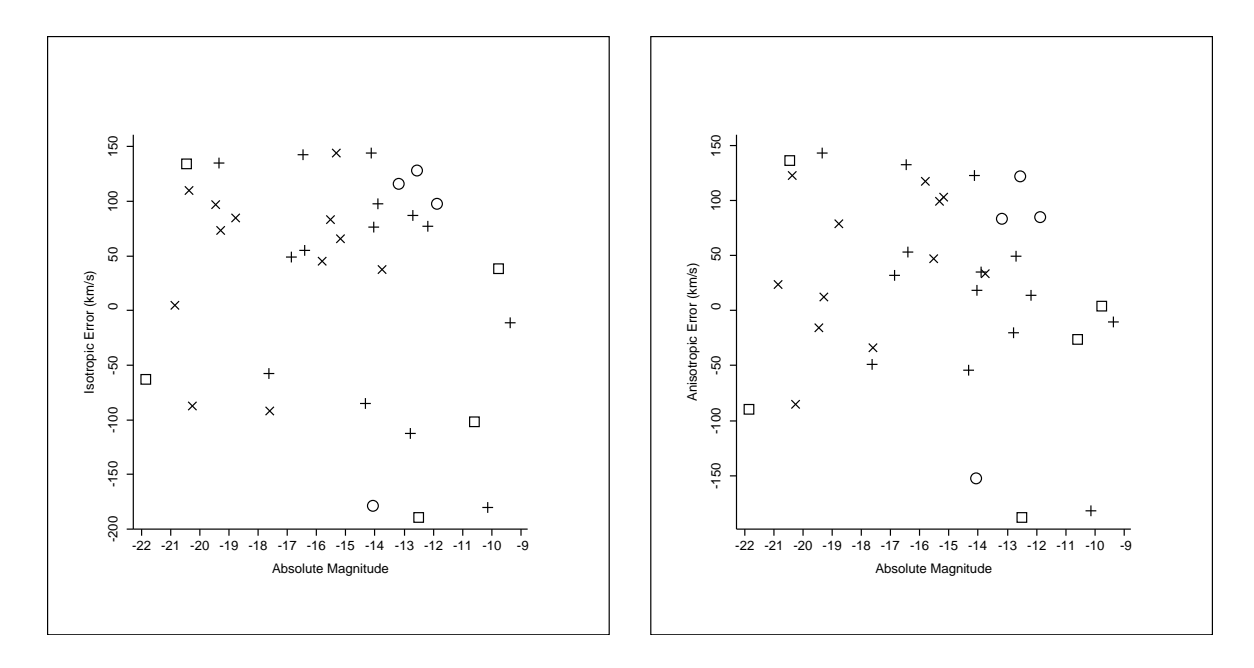


Fig. 17.— Deviation from (left) isotropic and (right) anisotropic Hubble expansion as a function of absolute magnitude for the 35-galaxy sample, using distances, photometry and extinction measurements from the literature. As before, crosses indicate spiral galaxies; plus, irregular; boxes, elliptical or lenticular; circles, other, peculiar or unclassified.

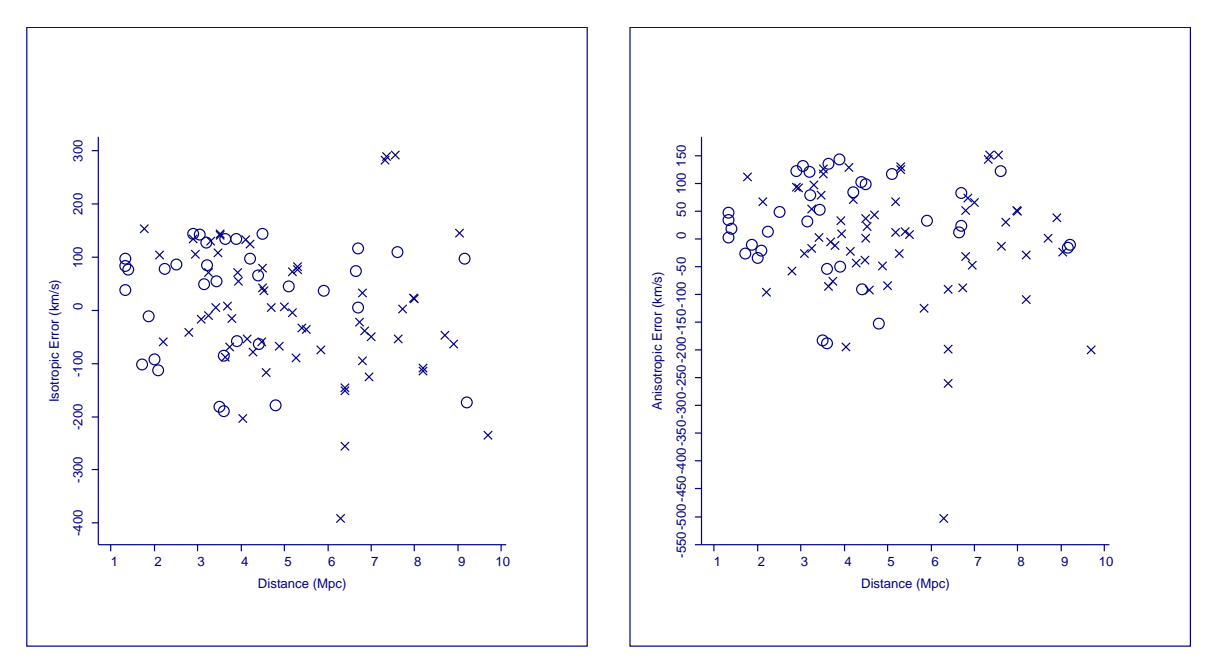


Fig. 18.— Deviation from (left) isotropic and (right) anisotropic Hubble expansion as a function of distance for the 97-galaxy sample. The galaxies with higher-quality distances are shown as open circles.

absolute magnitude -10 and -20 (for which extreme value there is no evidence). Then there should still be a change in dispersion by a factor of ten; while apparently there is none at all.

Searching for more sophisticated predictions, one quickly encounters one major problem with concentrating on the Local Volume: it is much smaller than the regions dealt with in studies of structure formation. In Jenkins et al. (1998), Figure 10, for instance (which shows predicted velocity dispersions for various length scales), a volume of 10 Mpc radius is beyond the small-scale edge of the curves drawn. One can extrapolate them, but the result is quite uncertain; they might predict a velocity dispersion of anywhere from 50 to 500 km s⁻¹.

Of more use for the question at hand, Inagaki, Itoh & Saslaw (1992) compared the analytic expression for velocity dispersion in Saslaw et al. (1990) with a series of n-body calculations. They found a rather small difference in rms velocity dispersion with mass: 169 compared to 179 (in scaled units) for sets of galaxies differing in mass by a factor of 100. However, they note that in their work the tendency for smaller galaxies to be affected more by gravitational interactions is offset by the tendency for larger galaxies to be found in rich clusters. Within the Local Volume there are no rich clusters. For such an effect to operate here, one would have to have groups made up of similarly-sized galaxies: dwarf groups and giant groups. This is certainly not true, each group in the Volume having galaxies with a wide distribution of size and brightness.

This brings us to the question of field and group galaxies. Inagaki, Itoh & Saslaw (1992) predict that field galaxies should have much smaller peculiar velocities than cluster galaxies. This is a quite plausible prediction: field galaxies should have little or no interactions which take them away from the Hubble flow, while group (and cluster) galaxies should be at least in the process of virializing. The situation with the present sample is shown in Figures 19 and 20.

There is no tendency for brighter galaxies to occur in groups, and no obvious tendency for group galaxies to have a larger velocity dispersion. To compare the situations quantitatively, we again use the dispersions about the models and employ (cautiously) the F-ratio test. For the 98-galaxy sample, isotropic model, the group dispersion is 120 km s⁻¹ against a field dispersion of 113 km s⁻¹. The F-ratio test gives a 64% significance to this; the difference is probably not significant. For the 98-galaxy anisotropic model the group dispersion is 93 km s⁻¹ against 122 km s⁻¹ for the field, giving a 95% significance—but with the *field* galaxies having a higher dispersion.

For the 35-galaxy isotropic model the field and group dispersions are 68 and 98 km s⁻¹, respectively, for a significance of 87%; the anisotropic model has 47 and 86 km s⁻¹ for 82%.

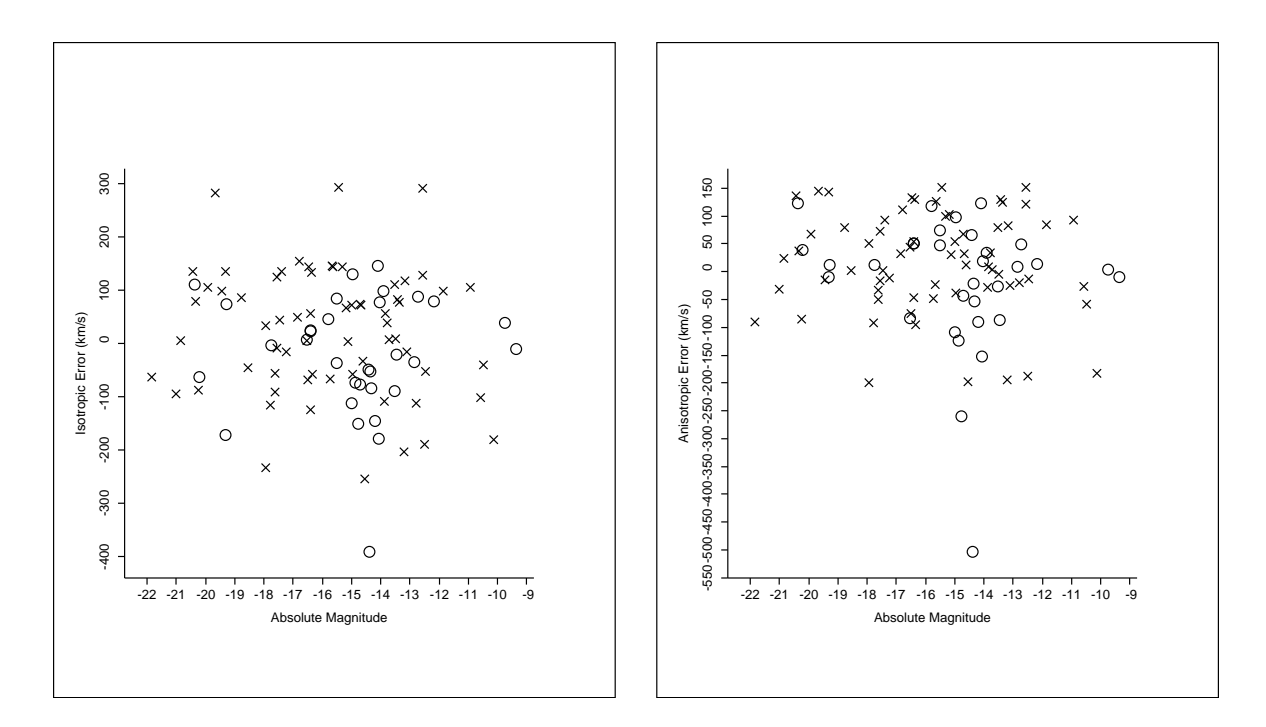


Fig. 19.— Deviation from (left) isotropic and (right) anisotropic Hubble expansion as a function of absolute magnitude for the 97-galaxy sample, using distances, photometry and extinction measurements from the literature. Crosses indicate galaxies in groups, circles field galaxies.

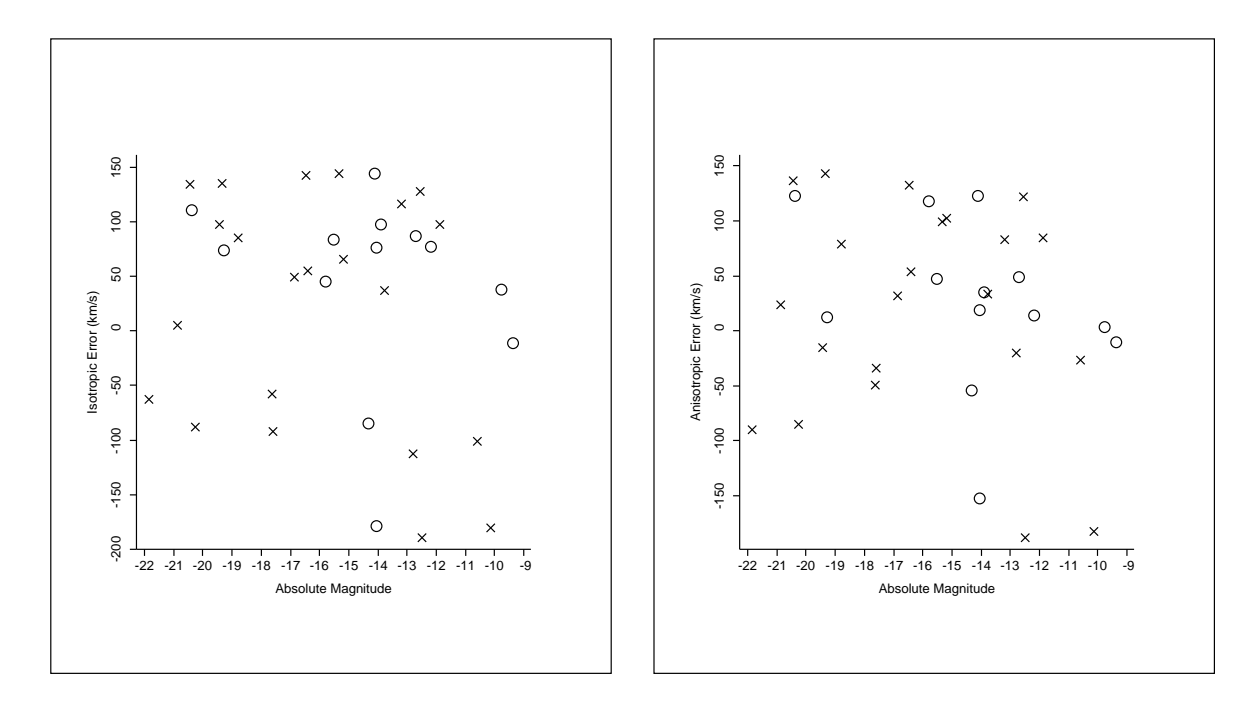


Fig. 20.— Deviation from (left) isotropic and (right) anisotropic Hubble expansion as a function of absolute magnitude for the 35-galaxy sample, using distances, photometry and extinction measurements from the literature. Crosses indicate galaxies in groups, circles field galaxies.

Here it appears that we have a true group versus field effect, and acting in the right direction. But these figures for significance are, as noted, to be treated cautiously. Also, with only 13 galaxies in the field category, we are hardly better off than Ekholm et al. (2001) from the standpoint of small-number statistics. I argue that an effect which appears only with a small sample of data (albeit one with better quality) and goes away (or reverses) with a larger sample is not real, especially in light of the quantitative unreliability of standard statistical measures when dealing with these samples.

The predictions of Inagaki, Itoh & Saslaw (1992) have been found to agree closely with observations on scales up to $50 \ h_{100}^{-1}$ Mpc (Raychaudhury & Saslaw 1996), as well as n-body calculations, so they may be taken to be well-established. Other techniques which match structure with motions on large scales also seem to work well (for example, those described in Courteau, Strauss, & Willick (2000)). On smaller scales, dynamical modeling of galaxy clusters and individual galaxies has become quite sophisticated and successful. In between, it appears, something different is happening.

4.3. Dynamics of the Peculiar Velocity Dispersion

A peculiar velocity distribution which ignores completely such things as absolute magnitude and the presence or absence of galaxy groups requires some explanation. The picture of motions generated by gravity, with that gravity field related to observable (luminous) matter in some simple way, does not appear to work in the Local Volume. There are a number of possible expanations:

- 1. Light does not trace mass, in that each observable galaxy is contained in a dark halo of about the same mass. Of course this contradicts otherwise successful simulations of large scale structure (for example, Springel et al. (2001); Mathis et al. (2002)). It is hard to see how the extreme variations in amounts of luminous matter (a factor of something like 10,000 over a ten-magnitude range) could come about within similar-sized halos. It is also hard to see how such a uniform field of dark matter halos themselves could come about. Alternatively, there could be a range of masses in dark matter halos, but no relation between their masses and the luminous matter within them; again, it is difficult to produce such a variation.
- 2. Light does not trace mass, in that the peculiar velocities of observable galaxies are produced by interaction with totally dark objects, which are so much more massive than galaxy halos that the latter are all equally affected by them. This has the attraction that such dark objects could be clustered similarly to galaxies on larger scales (allowing them to

define the Supergalactic Plane, for instance) and still not interfere with the internal dynamics of galaxy groups. It is difficult to understand, however, how the most massive dark matter objects could manage to avoid accreting any luminous matter at all.

- 3. The observed velocities of galaxies are not those of their dark matter halos; the luminous matter is "sloshing around" inside the dark potential well. This is probably a more attractive idea than the previous two, though a mechanism for such internal motion is lacking.
- 4. Peculiar velocities on this scale are not produced by gravitational interaction, but perhaps by some remnant of "primeval turbulence." This is an old idea in the context of the formation of galaxies. Heisenberg (in Hoyle (1949)) required some original motion in order for matter to clump together in galaxies; but this kind of motion is probably unimportant on galactic scales (Peebles 1993) (page 541).
- 5. We might have had bad luck with data, an unfortunate set of observations giving a misleading result of the sort that Ekholm et al. (2001) encountered. Of course this is harder to arrange with a much larger sample, and in particular it is hard to understand how the very even distribution of peculiar velocity with absolute magnitude could have been produced by any reasonable selection of data. It has indeed been argued above that the data sets at hand do not sample the true underlying dynamics well; but that is in the context of a particular model (isotropic or simple anisotropic expansion).
- 6. That idea leads on to the possibility that we are using the wrong kinematic model. There is indeed a general expansion of the Local Volume; but perhaps there is some different motion. This is a most attractive idea in that no current notions of cosmology or physics need necessarily be discarded or even greatly revised; however, it is not obvious to how to pursue it. The fact that no clear trend shows up in the plots of deviation versus the various spatial directions shows that no simple modification of the present models (including, for instance, a nonlinear effect of Virgocentric flow) is likely to be of use.

5. Summary

An examination of the kinematics of galaxies within 10 Mpc of the Milky Way has thrown up some surprises and one deep puzzle. An overall anisotropic expansion, expected from the distribution of galaxies in the Local Volume, can be calculated; but the uncertainty of its details and its strong dependence on the particular data set chosen indicate that it is not a useful description.

A mismatch between (on one hand) the calculated standard error of various model parameters and (on the other) the change of those parameters between data sets indicates that the present data do not form a good sample of the underlying kinematics, at least in the context of the models at hand. At least part of this is due to a selection bias against nearby galaxies with high radial velocities.

There is no variation in the width of the peculiar velocity dispersion with absolute magnitude over a range of ten magnitudes. Neither is there any apparent relationship with galaxy type, or between field and cluster galaxies. This is difficult to understand, as the tendencies which even out peculiar velocities among masses on larger scales are not at work. Mass may have no relation to light on these scales; or peculiar velocities might be produced by other than gravitational interactions among galaxies; or the set of data at hand might somehow be terribly misleading; or the reference kinematic model might be wrong.

To clarify the kinematics of this volume, and to shed light on (much less clear up) the puzzle, much additional data will be necessary. In particular, to define the shape of the peculiar velocity histogram many more galaxies need to be added. Unfortunately, accurate distances to objects between 2 and 10 Mpc require careful observations with the larger telescopes, and distances to a useful fraction of hundreds of galaxies will take much time to compile. It will be worthwhile to target, initially, bright and massive galaxies; those at high supergalactic latitude; those in the field; and those of high radial velocity but possibly still nearby.

It is a pleasure for the author to thank Donald Lynden-Bell for bringing the Hubble Tensor to his attention and for many helpful conversations. His debt to the indefatigable data collection efforts of Igor Karachentsev and his various coworkers should be evident in Table 1. The comments of an anonymous referee have very much clarified and improved this paper. This work has been supported in part by the Institute of Astronomy, University of Cambridge and in part by the Physics Department, U. S. Naval Academy.

REFERENCES

Aparicio, A., Dalcanton, J. J., Gallart, C. & Martínez-Delgado, D. 1997, AJ, 114, 1447

Aparicio, A., & Tikhonov, N. 2000, AJ, 119, 2183

Aparicio, A., Tikhonov, N., & Karachentsev, I. 2000, AJ, 119, 177

Axenides, M., & Perivolaropoulos, L. 2002, Phys. Rev. D, 65, 127301

- Baryshev, Yu. V., Chernin, A. D., & Teerikorpi, P. 2001, A&A, 378, 729
- Branchini, E., Teodoro, L., Frenck, C. S., Schmoldt, I., Efstathiou, G., White, S. D. M., Saunders, W., Sutherland, W., Rowan-Robinson, M., Keeble, O., Tadros, H., Maddox, S., & Oliver, S. 1999, MNRAS, 308, 1
- Bronshtein, I. N., & Semendyayev, K. A. 1998, Handbook of Mathematics (New York: Springer), English translation, reprint of third edition
- Crone, M. M., Schulte-Ladbeck, R. E., Hopp, U., & Greggio, L. 2000, ApJ, 545, 31
- ed. Courteau, S., Strauss, M. A., & Willick, J. 2000, ASP Conference Series 201, Cosmic Flows Workshop (San Francisco: ASP)
- Davidge, T. J., & van den Bergh, S. 2001, ApJ, 553, 133
- de Vaucouleurs, G., & Bollinger, G. 1979, ApJ, 233, 433
- de Vaucouleurs, G., de Vaucoulerus, A., Corwin, H. G. jr., Buta, R. J., Paturel, G., & Fouqué, P. (1991) Third Reference Catalogue of Bright Galaxies (New York: Springer-Verlag)
- Dekel, A., Eldar, A., Kolatt, T., Yahil, A., Willick, J. A., Faber, S. M., Courteau, S., & Burstein, D. 1999, ApJ, 522, 1
- Dolphin, A. E., Makarova, L., Karachentsev, I. D., Karachentseva., V. E., Geisler, D., Grebel, E. K., Guhathakurta, P., Hodge, P. W., Sarajedini, A., & Seitzer, P. 2001, MNRAS, 324, 249
- Drozdovsky, I. O., Schulte-Ladbeck, R. E., Hopp, U., Crone, M. M., & Greggio, L. 2001, ApJ, 551, 135
- Drozdovsky, I., & Karachentsev, I. D. 2000, A&ASupp., 142, 425
- Drozdovsky, I., & Tikhonov, N. 1999 in The Stellar Content of Local Group Galaxies, eds. Whitelock, P. & Cannon, R. (Provo, UT: Astronomical Society of the Pacific), 253
- Ekholm, T., Baryshev, Yu., Teerikorpi, P., Hanski, M. O., & Paturel, G. 2001, A&A, 368, L17
- Fall, S. M., & Jones, B. J. T. 1976, Nature, 262, 457
- Freedman, W. L., Madore, B. F., Gibson, B. K., Ferrarese, L., Kelson, D. D., Sakai, S., Mould, J. R., Kennicutt jr., R. C., Ford, H. C., Graham, J. A., Huchra, J. P., Hughes, S. M. G., Illingworth, G. D., Macri, L. M., & Stetson, P. B. 2001, ApJ, 553, 47

- Georgiev, Ts. B., Karachentsev, I. D., & Tikhonov, N. A. 1997, Astron. Lett. 23, 4
- Herrnstein, J. R., Moran, J. M., Greenhill, L. J., Diamond, P. J., Inoue, M., Nakai, N., Miyoshi, M., Henkel, C., & Riess, A. 1999, Nature, 400, 539
- Hoel, P. G. 1971, Introduction to Mathematical Statistics (Wiley: New York)
- Hoessel, J. G., Saha, A., & Danielson, G. E. 1998, AJ, 115, 573
- Hoyle, F. 1949, in Problems of Cosmical Aerodynamics, Burgers, J. M. & van der Hulst, N. C. eds. (Dayton: Central Air Documents Office), 28
- Inagaki, S., Itoh, M., & Saslaw, W. C. 1992, ApJ, 386, 9
- James, P. A., Joseph, R. D., & Collins, C. A. 1991, MNRAS, 248, 444
- Jenkins, A., Frenk, C. S., Pearce, F. R., Thomas, F. A., Colberg, J. M., White, S. D. M., Couchman, H. M. P., Peacock, J. A., Efstathiou, G., & Nelson, A. H. 1998, ApJ, 499, 20
- Jerjen, H., Freeman, K. C., & Ginggeli, B. 1998, AJ, 116, 2873
- Karachentsev, I. D., & Drosdovsky, I. O. 1998, A&ASupp., 131, 1
- Karchentsev, I. D., Sharina, M. E., & Huchtmeier, W. K. 2000, A&A, 362, 544
- Karachentsev, I. D., Karachentseva, V. E., Dolphin, A. E., Geisler, D., Grebel, E. K., Guhathakurta, P., Hodge, P. W., Sarajedini, A., Seitzer, P., & Sharina, M. E. 2000a, A&A, 363, 117
- Karachentsev, I. D., & Makarov, D. A. 1996, AJ, 111, 794
- Karachentsev, I. D., & Makarov, D. A. 2001, Astrophysics, 44, 1
- Karachentsev, I. & Musella, I. 1996, A&A, 315, 348
- Karachentsev, I. D., Sharina, M. E., Dolphin, A. E., Geisler, D., Grebel, E. K., Guharhakurta, P., Hodge, P. W., Karachentseva, V. E., Sarajedini, A., & Seitzer, P. 2001b, A&A, 379, 407
- Karachentsev, I. D., & Tikhonov, N. A. 1994, A&A, 286, 718
- Lahav, O., Santiago, B. X., Webster, A. M., Strauss, M. A., Davis, M., Dressler, A., & Huchra, J. P. 2000, MNRAS, 312, 166

Lee, M. G., & Byun, Y.-I. 1999, AJ, 118, 817

Lee, M. G., Freedman, W., & Madore, B. 1993, ApJ, 417, 553

Longmore, A. J., Hawarden, T. G., Webster, B. L., Goss, W. M., & Mebold, U. 1978, MNRAS, 183, 97p

Lynden-Bell, D., Faber, S. M., Burstein, D., Davies, R. L., Dressler, A., Terlevich, R. J., & Wegner, G. 1988, ApJ, 326, 19

Lynds, R., Tolstoy, E., O'Neil, E. J., & Hunter, D. A. 1999, AJ, 116, 146

Mathis, H., Lemson, G., Springel, V., Kauffmann, G., White, S. D. M., Eldar, A., & Dekel, A. 2002, MNRAS, 333, 739

Minniti, D., Zijlstra, A. A., & Alonso, M. V. 1999, AJ, 117, 881

Peebles, P. J. E. 1993, Principles of Physical Cosmology (Princeton: Princeton University Press)

Piotto, G., Capaccioli, M., & Pellegrini, C. 1994, A&A, 287, 371

Raychaudhury, S., & Saslaw, W. C. 1996, ApJ, 461, 514

Rubin, V. C., Ford, W. K. Jr., & Rubin, J. S. 1973, ApJ, 183, 111

Sakai, S., Madore, B. F. & Freedman, W. F. 1997, ApJ, 480, 589

Sakai, S., & Madore, B. F. 1999, ApJ, 526, 599

Sakai, S., & Madore, B. F. 2001, AJ, 555, 280

Sandage, A. 1986, ApJ, 307, 1

Saslaw, W. C., Chitre, S. M., Itoh, M. & Inagaki, S. 1990, ApJ, 365, 419

Schlegel, D. J., Finkbeiner, D. P. & Davis, M. 1998, ApJ, 500, 525

Schmidt, K.-H., & Boller, T. 1992, Astronomische Nachrichten, 313, 189

Schulte-Ladbeck, R. E., Hopp, U., Greggio, L., & Crone, M.M. 2000, AJ, 120, 1713

Schulte-Ladbeck, R. E., Hopp, U., Greggio, L., Crone, M. M., & Drozdovsky, I. O. 2001, AJ, 121, 3007

Sharina, M. E., Karachentsev, I. D., & Tikhonov, N. A. 1996, A&ASupp., 119, 499

- Soria, R., Mould, J. R., Watson, A. M., Gallagher, J. S. III, Ballester, G. E., Burrowws, C. J., Casertano, S., Clarke, J. T., Crisp, D., Griffiths, R. E., Hester, J. J., Hoessel, J. G., Holtzman, J. A., Scowen, P. A., Stapelfeldt, K. R., Trauger, J. T., & Westphal, J. A. 1996, ApJ, 465, 79
- Springel, V., White, S. D. M., Tormen, G., & Kauffmann, G. 2001, MNRAS, 328, 726
- Tikhonov, N. A., Galazutdinova, O. A., & Drozdovskii, I. O. 2000, Astrophysics, 43, 4
- Tolstoy, E., Saha, A., Hoessel, J. G., & Danielson, G. E. 1995a, AJ109, 579
- Tolstoy, E., Saha, A., Hoessel, J. G. & McQuade, K. 1995b, AJ, 110, 1640
- Tosi, M., Sabbi, E., Bellazzini, M., Aloisi, A., Greggio, L., Leitherer, C., & Montegriffo, P. 2001, AJ, 122, 1271
- Tully, R. B., & Fisher, J. R. 1987, Nearby Galaxies Atlas (Cambridge: Cambridge University Press)
- van de Weygaert, R., & Hoffman, Y. 2000, in Courteau, S., Strauss, M. A., & Willick, J. eds., 2000, ASP Conference Series 201, Cosmic Flows Workshop (San Francisco: ASP), 169
- Whiting, A. B., Hau, G. K. T., & Irwin, M. 2002, ApJS, 141,123
- Yahil, A. Tammann, G. A., & Sandage, A. 1977, ApJ, 217, 903

This preprint was prepared with the AAS IATEX macros v5.0.